LEBANESE AMERICAN UNIVERSITY

Damage and Life Cycle Assessment of New-Generation Wide-Base Tires in New Brunswick, Canada

By
Izak Said

A thesis
Submitted in partial fulfillment of the requirements
for the degree of Master of Civil and Environmental Engineering

School of Engineering
JULY 2017

LAU
الجامعة اللبنانية الأميركية
Lebanese American University

THESIS APPROVAL FORM

Student Name: Izak Said I.D. #: 200902030

Thesis Title : Damage and Life Cycle Assessment of New-Generation Wide-Base in New Brunswick, Canada

Program: Master of science in Civil and Environmental Engineering

Department: Civil Engineering

School: Engineering

The undersigned certify that they have examined the final electronic copy of this thesis and approved it in Partial Fulfillment of the requirements for the degree of:

Master of Science in the major of Civil and Environmental Engineering

Thesis Co-Advisor's Name	Dr. Caesar Abi Shdid	Signature	DATE: 14 / 7 / 2017 (Day / Month / Year)
Thesis Co-Advisor' Name	Dr. John Khoury	Signature	DATE: 14 / 07 / 2017 (Day / Month / Year)
Committee Member's Name	Dr. Imad Al Qadi	Signature	DATE: 14 / 07 / 2017 (Day / Month / Year)

LAU
الجامعة اللبنانية الأميركية
Lebanese American University

THESIS COPYRIGHT RELEASE FORM

LEBANESE AMERICAN UNIVERSITY NON-EXCLUSIVE DISTRIBUTION LICENSE

By signing and submitting this license, you (the author(s) or copyright owner) grants the Lebanese American University (LAU) the non-exclusive right to reproduce, translate (as defined below), and/or distribute your submission (including the abstract) worldwide in print and electronic formats and in any medium, including but not limited to audio or video. You agree that LAU may, without changing the content, translate the submission to any medium or format for the purpose of preservation. You also agree that LAU may keep more than one copy of this submission for purposes of security, backup and preservation. You represent that the submission is your original work, and that you have the right to grant the rights contained in this license. You also represent that your submission does not, to the best of your knowledge, infringe upon anyone's copyright. If the submission contains material for which you do not hold copyright, you represent that you have obtained the unrestricted permission of the copyright owner to grant LAU the rights required by this license, and that such third-party owned material is clearly identified and acknowledged within the text or content of the submission. IF THE SUBMISSION IS BASED UPON WORK THAT HAS BEEN SPONSORED OR SUPPORTED BY AN AGENCY OR ORGANIZATION OTHER THAN LAU, YOU REPRESENT THAT YOU HAVE FULFILLED ANY RIGHT OF REVIEW OR OTHER OBLIGATIONS REQUIRED BY SUCH CONTRACT OR AGREEMENT. LAU will clearly identify your name(s) as the author(s) or owner(s) of the submission, and will not make any alteration, other than as allowed by this license, to your submission.

Name: Ihab Said

Signature: [redacted]

Date: 04/07/2017

LAU
الجامعة اللبنانية الأميركية
Lebanese American University

PLAGIARISM POLICY COMPLIANCE STATEMENT

I certify that:

1. I have read and understood LAU's Plagiarism Policy.
2. I understand that failure to comply with this Policy can lead to academic and disciplinary actions against me.
3. This work is substantially my own, and to the extent that any part of this work is not my own I have indicated that by acknowledging its sources.

Name: Irak Said

Signature: [redacted]

Date: 04/07/2017

Dedication Page

TO MY LOVING PARENTS

ACKNOWLEDGMENT

First, I would like to thank my current committee members, Dr. John Khoury, Dr. Caesar Abi Shdid and Prof. Imad Al-Qadi, for their advice, encouragement and guidance throughout this study.

My sincere gratitude is also extended to my previous advisor Dr. Jean Chatila. I will forever be grateful for his support and guidance during my graduate studies at LAU. He has and will always be a great mentor to me and a person I look up to.

Special thanks go to Dr. Al-Qadi, who has been more than a committee member to me and working with him on this study has been a very enriching experience. He believed in me since day one and that made all the difference.

The completion of this work could not have been possible without the participation and assistance of Dr. Jaime Hernandez and Seunggu Kang. Their contribution is greatly appreciated and acknowledged.

To my parents, Melhem and Suzanne, I have no words to acknowledge the sacrifices they made for me. I am so blessed to have such a loving, supportive and selfless family.

Finally, I would like to acknowledge the financial support of the Department of Transportation and Infrastructure of New Brunswick, Canada.

Damage and Life Cycle Assessment of New-Generation Wide-Base Tires in New Brunswick, Canada

IZAK SAID

ABSTRACT

Wide-base tires (WBT) provide environmental benefits compared with conventional dual-tire assemblies (DTA), but research has consistently showed higher pavement responses and potential damage due to the use of WBT. Even though improvements were made with the introduction of new-generation wide-base tires (NGWBT) in 2000, NGWBT are still reported to be causing more damage to road infrastructure. However, a comprehensive evaluation of NGWBT and DTA considering the pavement damage and environmental benefits caused by each is not usually performed.

This study implements finite element method (FEM) analysis and life-cycle assessment (LCA) to perform a fair evaluation of the impact of NGWBT and DTA on the roads of New Brunswick. On one hand, the FEM analysis incorporates features usually omitted in conventional analysis of flexible pavements regarding material behavior (e.g., asphalt concrete viscoelasticity and granular material nonlinearity) and loading (e.g., moving load, three-dimensional nonuniform tire–pavement contact stresses). Critical pavement responses from the FEM model were input in a transfer function to calculate pavement damage. Two variables, combined DTA-to-NGWBT ratio and combined damage ratio, were utilized to assess both tire technologies from the impact on the pavement structure. On the other hand, LCA provided global warming potential (GWP) and energy consumption considering variables such as NGWBT market penetration, traffic level, and seasonal effect.

The highest impact difference between NGWBT and DTA on pavement structure was found near the surface, which could be related to near-surface fatigue cracking, while there was no difference on the subgrade rutting. After combining the distresses considered, pavement damage increased as NGWBT market penetration became greater; for a case study with market penetration of 20%, damage increment due to NGWBT increased by 8%. It has to be noted that the impact of steering wheel was not considered in this study, which usually causes the highest impact on pavements. An analysis tool was developed to ease the evaluation of the pavement and calculate pavement damage under any traffic, as well as base and subbase material.

Three scenarios were considered in the LCA analysis: i) Scenario 1: NGWBT and DTA resulted in the same bottom-up fatigue cracking and rutting potential; ii) Scenario 2: tires resulted in different cracking but the same rutting potential; and iii) Scenario 3: the tires resulted in the same cracking but different rutting potential. In general, the higher the NGWBT market penetration, the higher the environmental benefits due to the reduction in fuel consumption. Hence, a holistic assessment should be considered in the analysis of wide-base tire impact.

Keywords: Wide-base tires, Finite element method, Critical responses, Life cycle assessment, Global warming potential, Energy consumption.

TABLE OF CONTENTS

LIST OF FIGURES

LIST OF TABLES

CHAPTER 1:

INTRODUCTION

1.1 BACKGROUND

First-generation wide-base tires (FGWBT) were introduced in North America as an alternative to conventional dual-tire assembly (DTA) in the early 1980s. Initially, the trucking industry adopted FGWBT to improve fuel efficiency and increase hauling capacity. However, FGWBT, with width ranging from 385 to 425 mm., have proved to be more damaging to pavement infrastructure than conventional DTA. In response to this drawback, new-generation wide-base tires (NGWBT) were introduced in the early 2000s. NGWBT have a width ranging between 445 and 455 mm in North America, and even 495 mm in Europe; they are aimed to preserve the benefits of FGWBT while reducing pavement damage.

A fair and comprehensive comparison between NGWBT and DTA requires quantitative approaches to evaluate the potential increment in pavement damage and environmental impacts. Currently, the most practical approach to calculate pavement damage relies on transfer functions, which link critical pavement responses to the number of repetitions to failure; however, it may not recognize the impact of tire size or configuration. On the other hand, the most powerful, reliable, and versatile tool to calculate critical pavement responses is the finite element method (FEM). This analytical approach is able to accurately consider the contact between tire and pavement through the use of three-dimensional nonuniform contact stresses/forces and realistic contact area. Loading input has paramount importance when comparing NGWBT and DTA because both tires use different mechanisms to transfer a truck load to the pavement. In addition, FEM can account for various material models (e.g., linear viscoelastic, nonlinear stress dependent, inelastic), continuous moving load, and arbitrary temperature distribution. These features are far more realistic than the assumptions of

conventional flexibles pavement analysis, such as the ones used by the Mechanistic-Empirical Pavement Design Guide (MEPDG): static load, circular contact area, uniform contact stresses in the vertical direction only and equal to tire inflation pressure, and indirect consideration of viscoelastic materials.

New generation wide base tire is believed to provide environmental advantages over DTA. One of the environmental benefits of NGWBT is its relatively lower rolling resistance, which translates into lower fuel consumption and greenhouse gas emissions. Life-cycle assessment (LCA) quantifies the environmental benefits associated with material production, construction, and rehabilitation, equipment operation, pavement use phase, as well as pavement end of life. Therefore, a comparison of the environmental impact of using NGWBT in lieu of DTA is conducted.

Life cycle assessment and quantitative pavement response prediction allow a comprehensive comparison between NGWBT and DTA. Finite element analysis and LCA complement each other in the evaluation of the net impact of NGWBT compared with conventional DTA.

1.2 OBJECTIVE AND SCOPE

The main objective of this study is to compare NGWBT and conventional DTA in the province of New Brunswick, Canada, from two perspectives: pavement damage and environmental impact. The prediction of critical pavement responses is performed through advanced 3-D theoretical modeling. Responses from developed models are used in the assessment of both NGWBT and DTA on pavement performance and damage calculation for LCA. The comparison is limited to typical pavement structures in New Brunswick.

The general work plan of the study is presented in Figure 0-1. First, the information needed for the development of the pavement FEM models is gathered: material characterization, traffic, tire–pavement contact loads for both tires, and environmental

conditions. Second, simulation of the pavement structures and damage calculation is performed using the FEM. Python script was used for preparing input file and post-processing of results. Finally, the LCA is completed, thus allowing a comprehensive comparison between NGWBT and DTA.

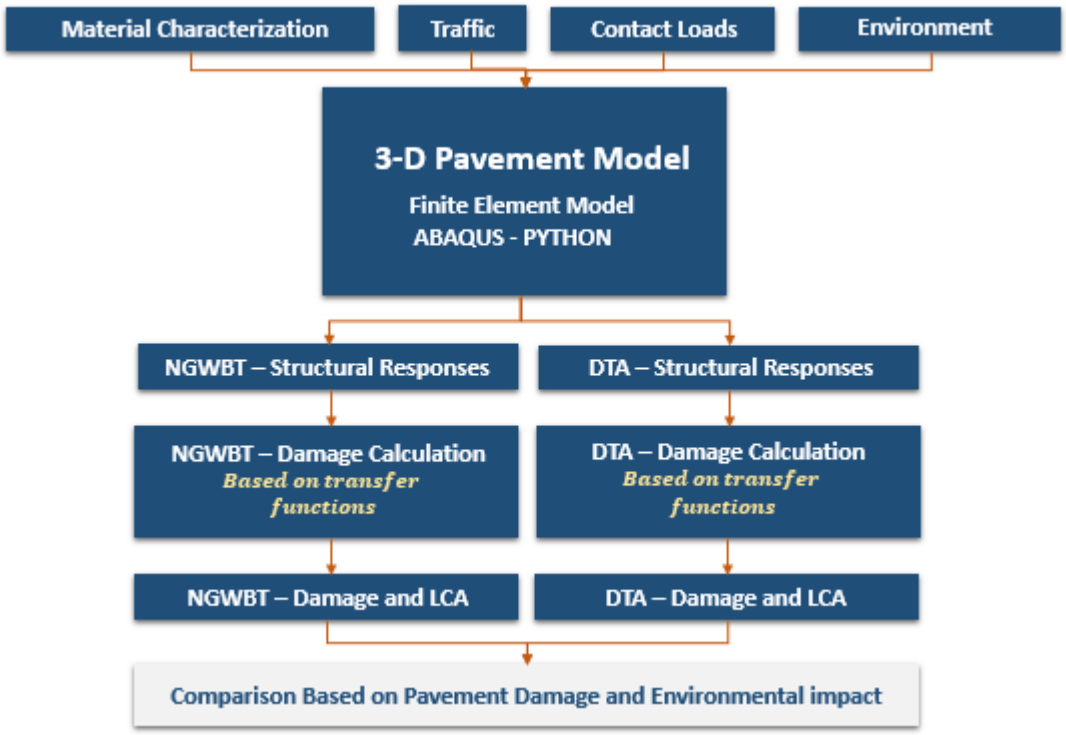

Figure 0-1. General steps in the assessment of DTA and NGWBT impact.

The objectives of this study include the following:

- Determine the impact of NGWBT and DTA on critical pavement responses and damage using FEM analysis. The FEM models include variables usually omitted in the conventional analysis of flexible pavement such as dynamic analysis, moving load, linear viscoelastic asphalt concrete (AC), nonlinear granular materials, 3-D contact loads, nonuniform temperature distribution in the AC layer, and interaction between pavement layers. Finite element analysis is used to

determine the critical pavement responses, which are maximum longitudinal tensile strains at the bottom of the AC, shear strain in each layer, and vertical strain in each layer

- Perform LCA analysis on the considered pavement structures to obtain a comprehensive evaluation of the impact of NGWBT and DTA. The evaluation is mainly focused on the material, construction, use phase, and maintenance stages. Various market penetrations of NGWBT and percentage of axles equipped with NGWBT are analyzed

1.3 RESEARCH SIGNIFICANCE

Wide-base tires are generally accepted as having significant potential benefits, including improved fuel economy, lower costs, and improved safety. This study is intended to quantify the impact of loaded tire on pavement damage using advanced theoretical modeling and evaluate the sustainability impact by performing full life cycle assessment to quantify energy usage and resulted emission from cradle to grave for typical pavement sections in New Brunswick. The significance of this research lies in applying a holistic evaluation of the impact of wide-base tires based on both pavement damage and environmental impact. Hence, allowing a quantitative assessment of the economic, environmental, and social impacts be determined when part of the DTA are replaced with NGWBT. Hence, providing the decision makers with the needed information for developing any new policies or permit fee schedules.

1.4 OVERVIEW OF THE STUDY

The body of this thesis consists of seven chapters and eight appendices. Chapter 2 provides a concise literature review where existing research regarding the effect of WBT on pavements is presented. Chapter 3 details the pavement sections and the model considered in this study, in addition to material characterization, environmental factors, temperature seasonal variation, and definition of 3-D contact loads for both NGWBT and

DTA. Chapter 4 focuses on the critical pavement responses and damage calculation; while LCA results are presented in Chapter 5. Chapter 6 describes the development of a tool that allows quick analysis. Finally, Chapter 7 includes the conclusions of the study. The thesis also includes eight appendices to provide detailed results and calculations.

CHAPTER 2:

LITERATURE REVIEW

Wide-base tires (WBT) usage has impact not only on pavement damage, but also on the environment. Since the 1980s, research efforts have focused on comparing pavement structural response between WBT and DTA. However, more recently, there has been increased interest in quantifying the environmental benefits of WBT for a holistic evaluation of both tire technologies.

Initially, NGWBT emerged as an alternative to FGWBT, which proved to be more damaging to pavements. Studies in Finland, Virginia, Pennsylvania, and California can be cited as examples of such findings. In Finland, FGWBT was compared with DTA, and it was found that FGWBT caused between 1.2 and 4 times more damage than DTA (Huhtala et al., 1989), with the difference decreasing as AC layer thickness increased (Huhtala, 1986). In Virginia, FHWA concluded that FGWBT created twice the rutting and 25% less fatigue life than DTA (Bonaquist, 1992). In addition, trucks traveling at 65 km/h increased pavement damage between 50 and 70% when using FGWBT in lieu of DTA (Sebaaly and Tabatabaee, 1992), and the number of repetitions for rutting failure in AC for FGWBT was between 10 and 60% the value for DTA (Harvey and Popescu, 2000). University of Florida showed that the number of repetition to reach 12.5 mm rutting at high temperature is the lowest for FGWBT 425 and the highest for DTA (Greene et al., 2009)

In Europe, several tire types were compared including NGWBT 495, FGWBT 385, DTA 315. Testing with different objectives in various countries showed that larger rutting was produced by FGWBT 385 (between 50 and 70% depending on pavement type), NGWBT 495 created 30% more rutting than DTA 315, and no significant difference was observed at the bottom of the AC if the pavement structure is very stiff (COST 334, 2001). However, NGWBT 495 performed better than DTA 295 in instrumented sections in Ohio (Xue and Weaver, 2015). Strain measurements on a 125-mm-thick AC pavement in

Canada provided similar magnitudes for NGWBT and DTA in the base during summer, but higher values for NGWBT during spring (Pierre et al., 2003). In some instances, similar responses were reported between the two tires, such as in a research performed by the National Center for Asphalt Pavement technology for tensile strains at the bottom of the AC and stress on top of the subgrade (Priest and Timm 2006). After combining various damage mechanisms, lower combined damage ratios where reported for NGWBT in Virginia (Al-Qadi et al., 2004; Al-Qadi et al. 2005a; Al-Qadi et al., 2005b; and Elseifi et al. 2006).

Accelerated pavement testing has been beneficial for comparing the two tire technologies at hand. This approach was used by researchers at University of Illinois to conclude that FGWBT 425 is more damaging than NGWBT 455 (Al-Qadi and Wang 2009a; Al-Qadi and Wang 2009b; Al-Qadi and Wang 2009c; and Dessouky et al., 2006). Similarly, experimental measurement in a pavement test track showed NGWBT creating 30% higher strains at the bottom of the AC (Grellet et al, 2012; Grellet et al., 2013).

Numerical models have also been used to predict pavement responses and study WBT and DTA. Multiple software has been implemented to compare pavement responses from WBT and DTA, including BISAR (Sebaaly and Tabatabaee, 1989), VESYS-DYN (Gillespie et al., 1992), CIRCLY (Perdomo and Nokes, 1993), and 3D-MOVE (Siddharthan et al., 2002). Besides consistently showing higher responses/damage for wide-base tires, numerical models highlighted the importance of the tire–pavement contact assumptions when comparing both tire technologies, mainly in regions close to the surface. The finite element software ABAQUS is the most versatile tool to accurate analyze pavement structure, and it has been used to continuously improve numerical representations of flexible pavement (Kim et al., 2009; Yoo et al., 2006; Elseifi et al., 2006; Al-Qadi and Yoo, 2007; Yoo and Al-Qadi, 2007; Yoo and Al-Qadi, 2008; Al-Qadi et al., 2010).

From an environmental point of view, it has been reported that the transportation sector is the second largest greenhouse gas (GHG) contributor after the oil and gas sector in Canada in 2014; and the operation of freight accounts for 32% of the transportation

sector (Environment and Climate Change Canada, 2016). The same reference showed that emissions from light trucks and freight trucks increased by 123% and 132%, respectively, between 1990 and 2014; indicating improving the fuel efficiency of trucks can significantly contribute to the GHG reduction.

New generation wide base tire provides considerable benefits in fuel efficiency (between 2 and 10%), hauling capacity, and ride comfort (Al-Qadi and Elseifi, 2008). GENIVAR (now rebranded WSP Global) found the net saving of NGWBT is $10.3 million per year when direct costs and benefits were considered. Based on the conducted survey, six of the seven firms in Québec experienced reductions in fuel consumption between 3.5% and 12% (GENIVAR, 2005). Franzese et al. (2010) found fuel economy improvement as the number of NGWBT on the Class 8 trucks increases; a 6% increase when either the tractor or the trailer is equipped with NGWBT and a 9% increase if both the tractor and the trailer are equipped with NGWBT. Ponniah et al. (2010) estimated 1.5% fuel economy improvement per axle after a thorough review of aforementioned studies. The U.S. Environmental Protection Agency (2016) and Michelin (2016) estimated fuel savings of 3% and up to 10%, respectively. Another study by Kang et al. (2017) used a 3.2% fuel saving for NGWBT for LCA analysis.

Earlier European pavement LCA studies (Häkkinen & Mäkelä, 1996; Stripple, 2001) evaluated the environmental impacts of tires on concrete and asphalt pavements. Meli (2006) conducted an LCA study on concrete and asphalt pavements in Canada. Research gaps in pavement LCA were studied by Santero (2009), and the impact of pavement surface characteristics, vehicle type, and traffic on rolling resistance (RR) was studied by Wang et al. (2012). Pavement LCA guideline (Van dam et al., 2015) and framework (Harvey et al., 2016) documents were recently published by the FHWA. However, the environmental impacts of using NGWBT in pavement LCA have not been extensively studied.

Greater pavement damages can cause earlier pavement deterioration, triggering more frequent pavement rehabilitation during its design life. Therefore, the LCA analysis

should be conducted to determine the net benefit of using NGWBT in the pavement LCA framework. In the present study, both pavement structural response and environmental impact are utilized to perform a comprehensive evaluation of NGWBT and DTA on road infrastructure in New Brunswick.

CHAPTER 3:

FINITE ELEMENT MODEL

This chapter describes the main components of the pavement finite element method (FEM) model: material properties, pavement temperature, and tire loading. For material properties, the model for each layer in the pavement structure is described. In addition, ambient temperature for each season and its variation through the AC layer are summarized. This section of the thesis describes the general configuration of the model regarding geometry and finite element types.

3.1 MATERIAL PROPERTIES

Three material behaviors were incorporated in the finite element model: linear viscoelasticity, nonlinear stress dependent, and linear elastic. Linear viscoelasticity was applied to AC based on 14 dynamic modulus test results reported in the Long-Term Pavement Performance (LTPP) database for sections in New Brunswick. The information was processed to calculated Prony series terms and Williams-Landel-Ferry constant, which were input in ABAQUS to model AC as linear viscoelastic. Figure 0-1 shows the master curve of the AC layer.

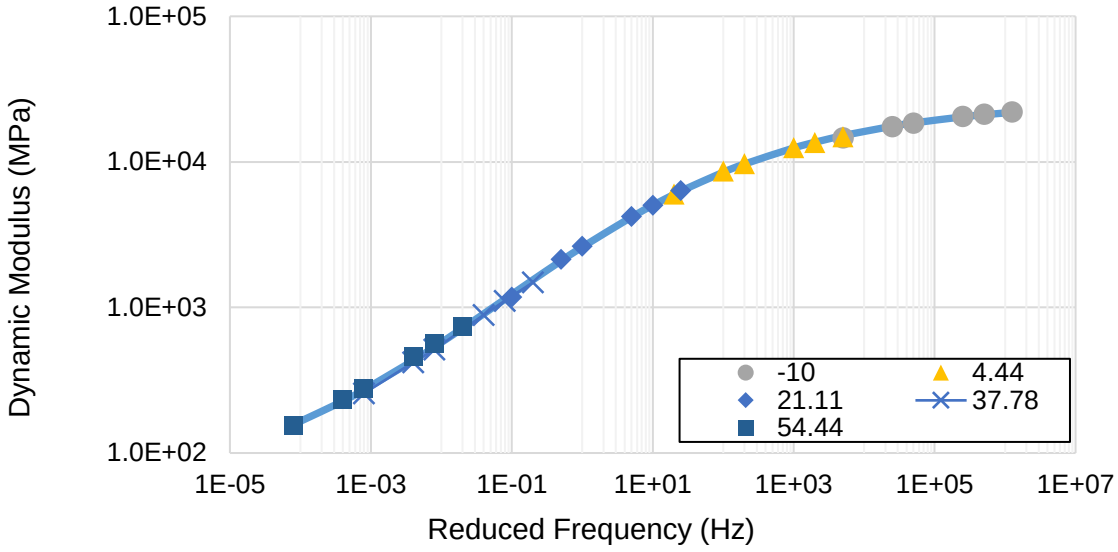

Figure 0-1. Master curve of asphalt concrete.

The resilient modulus for crushed rock and gravel bases were characterized as nonlinear (stress dependent) cross-anisotropic. Even though stress dependency and cross-anisotropy increase the complexity of the finite element model, they are relevant factors in calculating pavement responses when AC thickness is relatively small (Kim et al., 2005). Material constants in this model are calculated based on a resilient modulus test that applies pulse loads in the vertical and radial direction; a database of these laboratory measurements was utilized to characterize the base layers of this study (Tutumluer, 2008; Tutumluer and Thompson, 1998). Subbase, borrow, and subgrade materials were assumed to be linear elastic. All needed properties were selected from LTPP databases, except for the rock material, which was not part of New Brunswick pavement sections at the time the LTPP testing was performed.

3.2 PAVEMENT TEMPERATURE

Seasonal temperature variation must be considered when modeling flexible pavements because of its significant influence on AC behavior. New Brunswick is governed by a humid continental climate with a yearly temperature ranging from -8.3 to 17 °C. The temperatures considered in this study are defined based on the average temperature

variation per quarter as shown in Table 0-1. Finally, temperature distribution through the AC surface layer is determined based on an analytical one-dimensional temperature distribution model (Wang et al., 2009).

Table 0-1. Quarterly Temperature Distribution on New Brunswick

Month	Season	Avg. Temperature (°C)
September	Fall	7
October		
November		
December	Winter	-8.3
January		
February		
March	Spring	3.3
April		
May		
June	Summer	17
July		
August		

3.3 LOAD CALCULATION AND DISTRIBUTION

A NGWBT and DTA loaded at 4500 kg with a tire inflation pressure of 690 kPa were considered (see Figure 0-2). The contact forces were based on earlier measurements by the Council for Scientific and Industrial Research in South Africa using the Stress-In-Motion system (De Beer and Fisher, 2013; Hernandez et al., 2013). Critical pavement responses, mainly close to the surface, are affected by the non-uniformity and three-dimensionality of tire–pavement contact loads (Al-Qadi and Yoo, 2007). In addition, NGWBT and DTA have very different load transfer mechanisms, so accurate comparison of pavement damage from both tires requires realistic loading characterization.

Figure 0-2. Tested NGWBT (left) and tested DTA (right).

Figure 0-3 shows a representative variation of the contact loads in the vertical, transverse, and longitudinal direction along the contact length for both tires; the figure only presents values at a specific location across the tire. As can be seen, NGWBT exhibits higher vertical contact stresses. In addition, previous analyzes have shown that contact area is higher for DTA (Hernandez et al., 2013). For the selected location, there are not significant difference in the longitudinal and transverse direction (around the tire center for both tires)

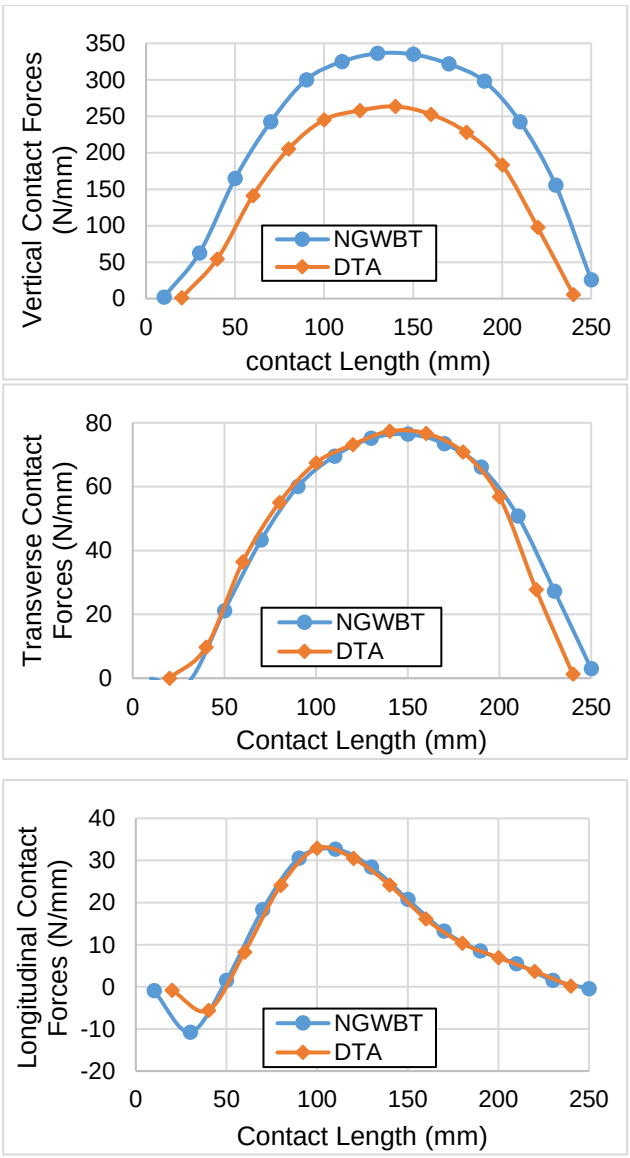

Figure 0-3**. Variation of vertical, transverse, and longitudinal contact forces along contact length.**

3.4 FINITE ELEMENT MODEL

The developed models were previously implemented for comparing NGWBT and DTA (Hernandez et al., 2016), including factors usually omitted in the conventional analysis of flexible pavements, which proved to be relevant when calculating critical pavement responses. The factors include: dynamic analysis (Yoo and Al-Qadi, 2007), continuous moving load (Yoo et al., 2006), nonuniform 3D contact stresses (Al-Qadi and Yoo, 2007),

nonuniform temperature distribution in the AC layer, interaction between pavement layers (Yoo et al., 2006), and infinite boundary elements.

The pavement model and the geometric configuration are shown in Figure 0-4. The model geometry consists of a wheel path, two transition zones ($L1$-$B1$ and $L2$-$B2$), and infinite elements. In the transition zone, the elements size is changes from small in the wheel path to coarse in the boundary. The size and type of finite element were determined by a mesh sensitivity analysis, comparing results from a finite element model with a multi-linear elastic solution. The main objective of the mesh sensitivity analysis is to find the coarsest mesh (low computational time) that provides accurate results. It should be highlighted that this simplified version of the pavement model was exclusively used to determine dimensions and finite element configuration; critical pavement responses were calculated using a full 3-D model that considered the variables described in the previous paragraph. Model validation (i.e., comparison between computer predicted and measured pavement responses) was performed in previous studies following the same modeling approach as in this study (Gungor et a., 2016).

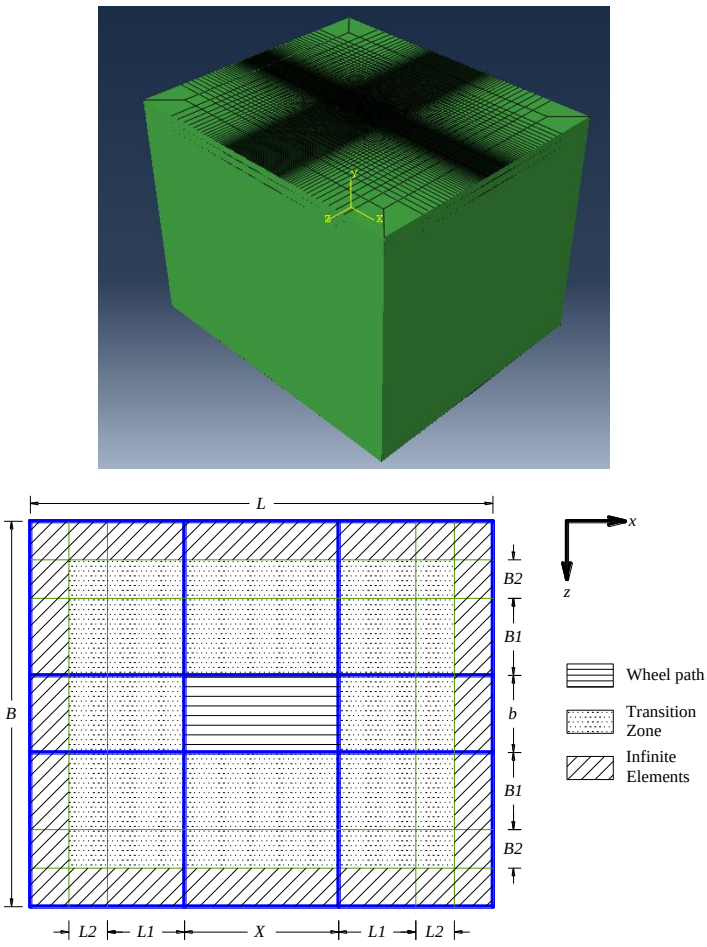

Figure 0-4. Pavement model using ABAQUS (left) and geometric configuration in plan view (right).

CHAPTER 4:

CRITICAL PAVEMENT RESPONSES AND PAVEMENT DAMAGE

4.1 PAVEMENT STRUCTURES AND ANALYSIS MATRIX

The pavement sections considered are arterial highways making a full loop around New Brunswick, Canada, passing through a wide variety of subgrade soils and bedrock types. The comparison is limited to three pavement structures, all with the same AC thickness (140 mm), a granular base of 150 mm, a subbase of 450 mm, on top of a 600-mm-thick layer of Borrow "A" material and a glacial till. The difference between the three sections lies in the material properties of the base and subbase: Section 1 has a crushed rock base and subbase; Section 2 has crushed gravel base and subbase; and Section 3 has crushed gravel base and crushed stone subbase. Section 1 represents the new highway standard section of New Brunswick; while Sections 2 and 3 represent old pavement sections. Figure 0-1 shows the configuration of the sections considered in this study.

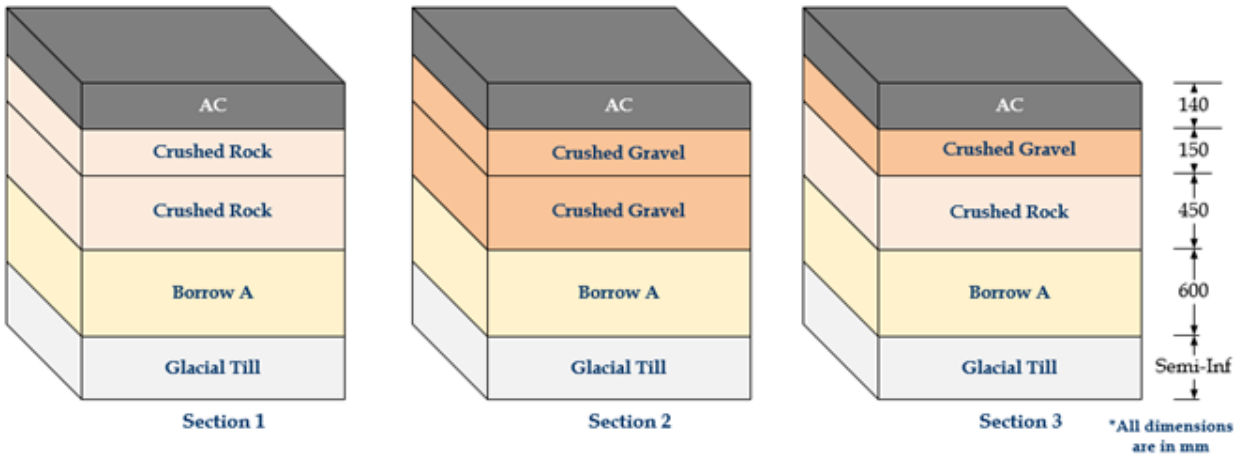

Figure 0-1. Sections considered in the analysis.

Due to the lack of information to properly match crushed rock with the available database, an alternative approach was implemented where base and subbase were categorized in three groups depending on their resilient modulus: weak, medium, and strong. Crushed gravel was identified as having medium resilient modulus, so five possible base–subbase combinations cover Sections 1, 2, and 3: weak–weak, medium–medium, strong–strong, medium–weak, and medium–strong. The subbase was assumed linear elastic modulus of 414 MPa (strong base), 287 MPa (medium base), and 137 MPa (weak base).

The finite element matrix included the combination of four seasons (fall, winter, spring and summer), two tire configurations (NGWBT and DTA), and five base–subbase combinations, thus rendering 40 finite element models.

4.2 CRITICAL PAVEMENT RESPONSES

Critical pavements responses are the ones linked to specific distresses through transfer functions. The critical pavement responses of interest in this study are tensile strain at the bottom of the AC, vertical strain on top of subgrade, and shear strain in the AC layer. The analyses were conducted for NGWBT and DTA; the steering wheel was not considered.

4.2.1 Tensile Strain at the Bottom of the AC

The variation of the tensile strain at the bottom of the AC ($\varepsilon_{11,ac}$) for a strong base–subbase combination is shown in Figure 0-2. NGWBT created between 16 and 18% higher tensile strain at the bottom of the AC layer as compared to DTA. This can be explained by the lower contact area and higher contact loads for NGWBT. Regarding the effect of temperature, the tensile strain at the bottom of the AC increased with increasing temperature. This behavior is expected because the stiffness of the AC layer decreases as the temperature becomes higher. It was also noticed that the effect of temperature on $\varepsilon_{11,ac}$ becomes minimal for lower magnitudes (e.g., winter vs. spring). The percentage increases in the response for DTA from winter to spring is 0.9%, which is

significantly lower than 42.2%, the change from spring to summer. The variation between the same seasons for NGWBT are 0.8 and 43.0 %.

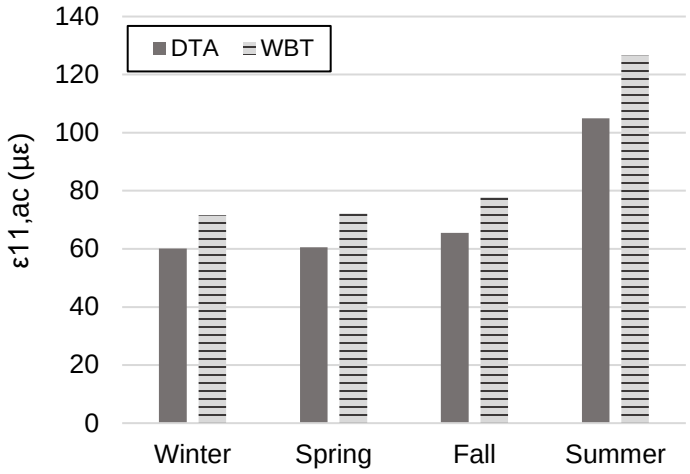

Figure 0-2. Tensile strain at bottom of AC for different temperatures, tire configuration, and strong base–subbase combination.

4.2.2 Vertical Strain on Top of the Subgrade

As observed in Figure 0-3, NGWBT and DTA caused almost the same vertical strain on top of the subgrade ($\varepsilon_{22,sg}$); the maximum percentage difference between the two tires is 1.7%. The negligible difference is caused by the lack of influence of contact loads distribution deep inside the pavement structure. Moreover, the comparison between responses of different seasons shows that temperature impact is minimal because it mainly influences AC layer. The influence vanishes in the subgrade, which is more than 1 m underneath the surface.

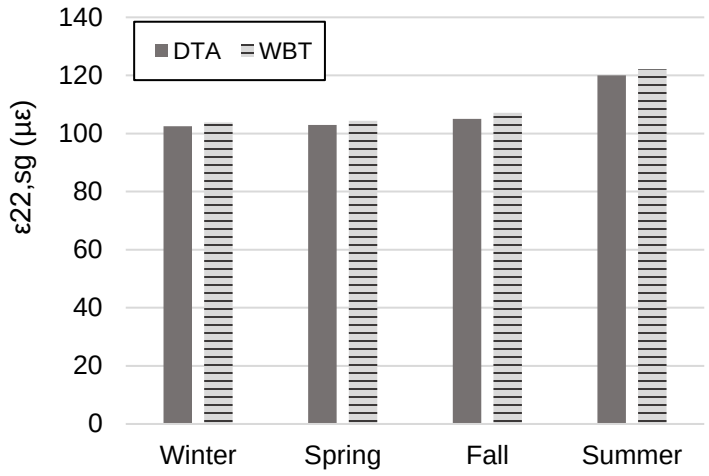

Figure 0-3. Maximum vertical strain on top of the subgrade for different temperatures, tire configuration, and strong base–subbase.

4.2.3 Shear Strain in AC

Using smaller contact area to transfer load from truck to pavement can also explain higher shear strain values for NGWBT; shear strain was around 20% higher for NGWBT (see Figure 0-4). As previously mentioned, NGWBT creates deeper deformations basin, so the distortion, which is directly related to shear strain, is higher. It is also noted that, as in the other critical pavement responses, the highest seasonal effect occurs between fall and summer, and there are no relevant changes between the other seasons.

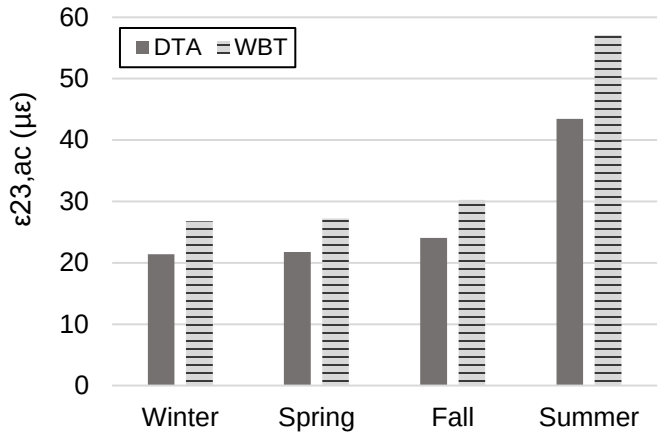

Figure 0-4. Shear strain in AC layer for different temperatures, tire configuration, and strong base–subbase.

Previous analysis corresponds to the strong base–subbase combination; similar trends were observed for the other base–subbase combinations. Table 0-1 presents the percentage increment of the specified response for the weak combination compared to strong. For instance, the first value in the table indicates that during fall season, the tensile strain at bottom of the AC increased 10.6% when the base–subbase combination changed from strong to weak. The increments varied between 3.5% for $\varepsilon_{23,ac}$ and NGWBT during winter and 16.1% for $\varepsilon_{11,ac}$ and DTA during summer. It was noted that the higher changes were seen for tensile strain at the bottom of the AC and the highest temperature. The actual values of all critical pavement responses, pavement sections, and seasons are presented in Appendix A.

Table 0-1. Percentage Increase in Pavement Responses due to Change in Materials Properties

		$\Delta\varepsilon_{11,botac}$ (%)	$\Delta\varepsilon_{22,sg}$ (%)	$\Delta\varepsilon_{23,ac}$ (%)
Fall	**DTA**	10.6	6.6	5.5
	WBT	9.8	6.2	4.2

Spring	**DTA**	9.5	5.8	5.2
	WBT	8.7	5.9	3.7
Summer	**DTA**	*16.1*	10.3	9.1
	WBT	14.6	10.5	4.7
Winter	**DTA**	9.1	5.8	4.6
	WBT	8.4	5.9	3.5

4.3 COMBINED DAMAGE RATIO

Four pavement distresses were considered: bottom-up fatigue cracking, near-surface fatigue cracking caused by near-surface shear strain, AC rutting, and subgrade rutting. Each of the critical pavement responses is linked to a failure mechanism through transfer functions as follows: tensile strain at the bottom of the AC is associated with bottom-up fatigue cracking, shear strain is related to near-surface fatigue cracking, and AC and subgrade rutting greatly depend on the vertical strains. Equations to calculated the number of repetitions to failure for each pavement distress are presented in Appendix B. The ratio between the number of repetitions to failure caused by both tires can be calculated as follows:

$$DW = \frac{N_{DTA}}{N_{WBT}} \tag{0-1}$$

where DW is the ratio of number of repetitions to failure between DTA and NGWBT for a specific distress; N_{DTA} is the allowable number of loading repetitions for DTA; and N_{NGWBT} is allowable number of loading repetitions for NGWBT. Consequently, four DW values can be calculated: DW_{BU} for bottom-up fatigue cracking, DW_{TDS} for near-surface cracking caused by shear strain in the AC, DW_{RS} for subgrade rutting, and DW_{RH} for rutting in the AC layer.

Figure 0-5 shows the ratios for strong base and subbase and all the seasons. The highest ratio between the seasons was 3.1 and was observed for near-surface cracking caused by shear strain. Conversely, subgrade rutting showed the lowest ratio with an average

of 1.07, agreeing with the fact that the influence of contact loads decreased with depth. Similar trends and ratios, which are presented in Appendix C, were found for the other base and subbase materials

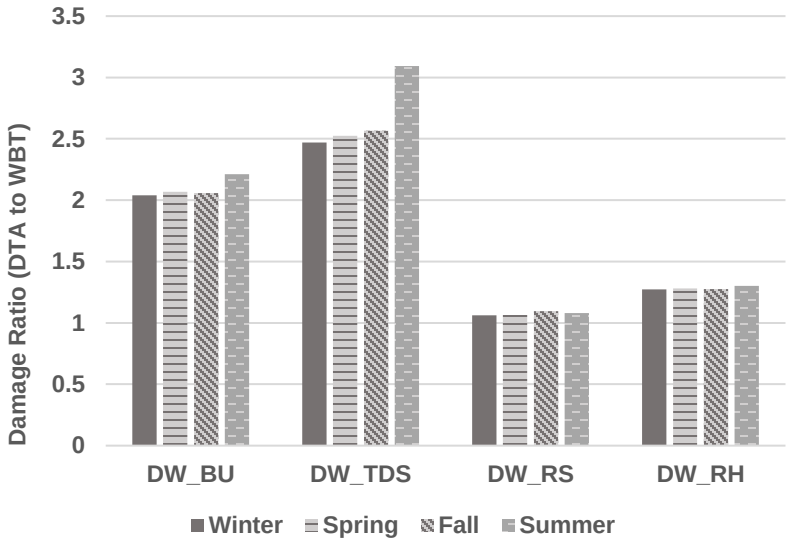

Figure 0-5. Damage ratio for considered distresses and seasons and strong base and subbase.

The values in Figure 0-5 assume that there is no interaction between various failure mechanisms in the pavement, which is unrealistic. The failure mechanisms considered were combined using a logarithmic weighting factor. This is especially beneficial as the variables to be integrated spread over several orders of magnitude. The combined NGWBT to DTA ratio can be calculated using the following equation (Al-Qadi et al. 2004):

$$CDW = a_1 DW_{BU} + a_2 DW_{TDS} + a_3 DW_{RS} + a_4 DW_{RH} \quad (0\text{-}2)$$

$$a_i = \frac{\frac{1}{\log(N_i)}}{\sum_{j=1}^{m} \frac{1}{\log(N_j)}} \quad (0\text{-}3)$$

where: CDW is the combined DW ratio, DW_{BU} is the WD ratio for bottom-up fatigue cracking, DW_{TDS} is the WD ratio for near-surface cracking caused by shear strain, DW_{RS} is the WD ratio for subgrade rutting, DW_{RH} is the WD ratio for AC rutting, and m is the

total number of failure mechanisms considered. Figure 0-6 presents a summary of CDW values for the analysis matrix, where the horizontal axis indicates the base and subbase material (S: strong, M: medium, and W: weak). It can be observed that, even though the responses vary greatly from one season to the other, CWD is relatively consistent. However, summer provided higher cumulative ratios.

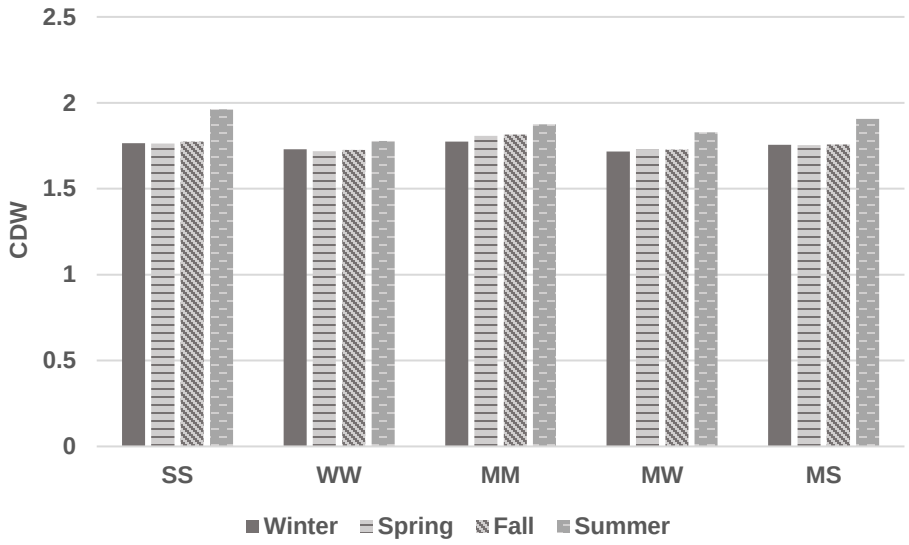

Figure 0-6. Cumulative damage ratio.

It should be noted that the damage ratios reported assume that, for the same pavement section, all traffic is changed from DTA to WBT, which is unrealistic. To address this issues, the following approach was used to include various percentage of NGWBT usage in the roads of New Brunswick.

4.4 DAMAGE DUE TO TRAFFIC

The combined DW ratio compares the number of repetitions to failure from NGWBT and DTA. If used to compare the effect of the two tires on pavements, CDW indirectly assumes that the same road is subjected exclusively to either NGWBT or DTA, which is unfeasible. A procedure to consider various market penetration of NGWBT is presented

in this section; the procedure is based on reducing the number of load repetitions a pavement can withstand when subjected to NGWBT. Based on the cumulative damage theory, the yearly damage for a distress can be written as follow:

$$D = \sum_{i=1} \frac{n_i}{N_i} = \frac{n_{fa}}{N_{fa}} + \frac{n_{wt}}{N_{wt}} + \frac{n_{sm}}{N_{sm}} + \frac{n_{sp}}{N_{sp}} = \frac{n}{N} \quad (0\text{-}4)$$

where n_i: number of load applications in season i

N_i: number of load applications to cause failure in season i

$i = fa, wt, sp,$ and sm: fall, winter, spring, and summer, respectively

n: number of load applications in the design period

N: effective number of repetitions to failure

Assuming that the traffic in the design period can be equally divided between the seasons and using Eq. (4.4), the effective number of repetitions to failure for each distress can be calculated as follows:

$$N_j = \frac{4}{\sum \frac{1}{N_{i,j}}} = \frac{4}{\frac{1}{N_{fa,j}} + \frac{1}{N_{wt,j}} + \frac{1}{N_{sm,j}} + \frac{1}{N_{sm,j}}} \quad (0\text{-}5)$$

where $j = BU, TDS, RS,$ and RH indicates the distress type (BU bottom-up fatigue cracking, TDS for near-surface cracking caused by shear strain, RS for subgrade rutting, and RH ratio for AC rutting). The number of load applications to failure in each season and distress $N_{i,j}$ is calculated using the equations in Appendix B and responses presented in section 4.2. The combined number of repetitions to failure that includes market penetration can be calculated using the following equation:

$$N_j = C_{WBT} \times N_{WBT,j} + (1 - C_{WBT}) \times N_{DTA,j} \quad (0\text{-}6)$$

where: $C_{WBT} = w \times PA_{WBT}$: NGWBT contribution coefficient

N_j: number of repetitions to failure for distress j

w: market penetration percentage (%)

PA_{WBT}: percentage axles with wide-base tires (%)

$N_{DTA,j}$: number of repetitions to failure by DTA for distress j

$N_{WBT,j}$: number of repetitions to failure by NGWBT for distress j

On the other hand, to calculate the total number of load applications, the following equation is used (AASHTO method):

$$ESAL = 365 \times AADT_{t=0} \times T \times T_f \times GY \times D \times L \quad (0\text{-}7)$$

where $ESAL = n$: equivalent single axle load or number of load repetitions

$ADT_{t=0}$: average annual daily traffic at time t = 0

T: percentage of trucks

T_f: truck factor

GY: growth factor for a specific number of years

D: directional distribution factor

L: lane distribution factor

Note that including NGWBT in the traffic calculation is not feasible because of the lack of truck factor for such tires. The growth factor is computed as follows:

$$GY = \frac{(1+r)^Y - 1}{r} \quad (0\text{-}8)$$

where GY: growth factor

r: growth rate

Y: number of years of interest

Finally, the cumulative damage ratio for the four distresses considered in this study is calculated as follow:

$$CDR = a_1 \frac{n}{N_{BU}} + a_2 \frac{n}{N_{TDS}} + a_3 \frac{n}{N_{RS}} + a_4 \frac{n}{N_{RH}} \quad (0\text{-}9)$$

$$a_k = \frac{\frac{1}{\log(N_k)}}{\sum_{i=1}^{m} \frac{1}{\log(N_i)}} \quad (0\text{-}10)$$

where: CDR= combined damage ratio

N_{BU}= repetitions to failure for bottom-up fatigue cracking

N_{TDS}= repetitions to failure for near-surface cracking caused by shear strain

N_{RS}= repetitions to failure for subgrade rutting

N_{RH}= repetitions to failure for AC rutting

m= total number of failure mechanisms considered

4.5 EXAMPLE OF DAMAGE DUE TO TRAFFIC

The objective of this solved example is to show a step-by-step procedure of how to calculate the cummualtive damage ratio of a pavement struture with thickness shown in Figure 0-1. The inputs to this application are as follows:

- Modulus of base: 414 MPa (strong nonlinear base)
- Modulus of subbase: 414 MPa
- Analysis period: 30 Years
- Market penetration: 10%
- Percent of axles with Wide-base Tire: 50%
- Directional AADT: 7000
- Growth rate: 1%
- Truck percent: 20 %
- Truck factor: 0.69
- Lane distribution factor: 0.5

Step I: Calculate critical pavement responses ($\varepsilon_{11,botac}$, $\varepsilon_{22,sg}$, $\varepsilon_{23,ac}$, and $\varepsilon_{22,ac}$) for both tires and four seasons using the finite element model. Table 0-2 shows all the critical pavement responses collected for the calculation of CDR.

Table 0-2: Responses Needed for the Calculation of Combined Damage Ratio

		Pavement Responses (Micro-Strain)			
Season	**Tire**	$\varepsilon_{11,botac}$	$\varepsilon_{22,sg}$	$\varepsilon_{23,ac}$	$\varepsilon_{22,ac}$
Fall	DTA	65.68	105.00	24.08	-
	NGWBT	78.08	107.15	30.26	-
Winter	DTA	60.33	102.50	21.43	-
	NGWBT	71.82	103.88	26.78	-
Spring	DTA	60.85	102.90	21.76	-
	NGWBT	72.43	104.34	27.27	-
Summer	DTA	104.62	120.00	43.37	-
	NGWBT	126.22	122.10	56.91	-

Step II: Calculate the total number of repetitions to failure for each distress, tire configuration, and season using the transfer functions in Appendix B. Table 0-3 summarizes all calculated N_f.

Table 0-3: Number of Repetitions to Failure for the Calculation of Combined Damage Ratio

Season	**Tire**	N_{BU}	N_{RS},	N_{TDS}	N_{RH}
Fall	DTA	5.57×10^{9}	8.88×10^{8}	2.11×10^{8}	2.17×10^{9}
	NGWBT	2.67×10^{9}	8.11×10^{8}	8.12×10^{7}	1.70×10^{9}
Winter	DTA	2.04×10^{9}	9.89×10^{8}	8.76×10^{7}	7.22×10^{10}
	NGWBT	1.001×0^{9}	9.31×10^{8}	3.54×10^{7}	5.67×10^{10}
Spring	DTA	5.11×10^{9}	9.72×10^{8}	2.13×10^{8}	4.41×10^{9}
	NGWBT	2.44×10^{9}	9.13×10^{8}	8.33×10^{7}	3.43×10^{9}
Summer	DTA	2.57×10^{9}	4.88×10^{8}	6.00×10^{7}	1.85×10^{8}
	NGWBT	1.15×10^{9}	4.52×10^{8}	1.93×10^{7}	1.42×10^{8}

Step III: Using Eq. (4-5), calculate the effective number of repetitions to failure (combination of all seasonal N_f) for each distress. The output of this equation is shown in Table 0-4.

Table 0-4: Effective Number of Repetitions to Failure for Different Distresses and Tire Configurations

		N_{BU}	N_{RS},	N_{TDS}	N_{RH}
Tire	DTA	5.57×10^{9}	8.88×10^{8}	2.11×10^{8}	2.17×10^{9}
	NGWBT	2.67×10^{9}	8.11×10^{8}	8.12×10^{7}	1.70×10^{9}

Step IV: Using Eq. (4-6), compute the combined number of repetitions to failure that includes market penetration. At this step, each distress will have one number of repetitions to failure. The combined number of repetitions to failure for the five distresses considered in this example are: N_{BU} = 3.72×10^{9}; N_{RS} = 8.31×10^{8}; N_{RH} = 1.95×10^{10}; and N_{TDS} = 1.39×10^{8}.

Step V: Finally, all distresses are combined using Eq. (4-9) and (4-10). The CDR for the case in this example is 0.01.

Using the New Brunswick Pavement Analysis Tool (NBPAT), which is introduced and described in Chapter 6, the effect of different market penetrations and AADTs on the cumulative damage ratio (CDR) was calculated. The example includes an AADT of 7000 and multiple market penetrations. The market penetration varied from 0 to 100% with increments of 5%. The effect of NGWBT market penetration on CDR is shown in Figure 0-7. As expected, results show that higher market penetration causes more damage to the pavement and that the rate of pavement deterioration increases with increasing market penetration.

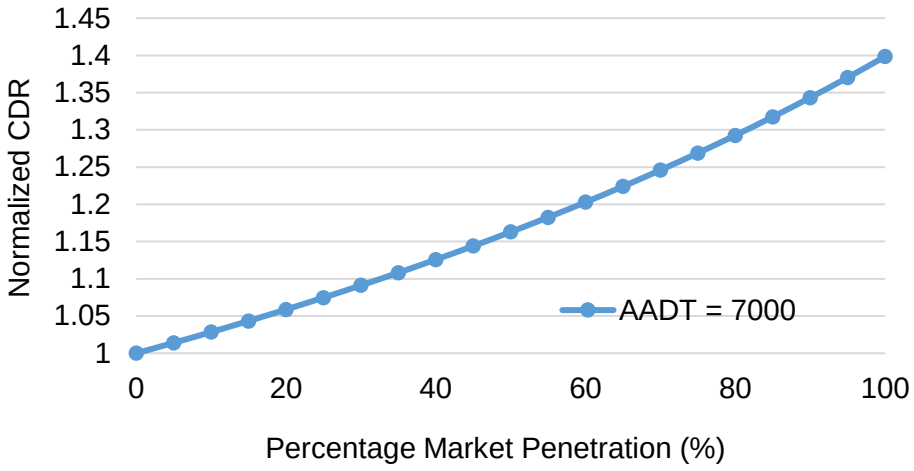

Figure 0-7: Effect of NGWBT market penetration on CDR.

CHAPTER 5:

LIFE-CYCLE ASSESSMENT

Life-cycle assessment (LCA) is a technique widely adopted for quantifying the environmental impacts of a product or a system during its life cycle. In this section, LCA is performed to achieve the following objectives: i) develop a methodology analyzing the interaction between NGWBT and pavements; ii) evaluate the effect of new-generation wide-base tire on energy consumption and global warming potential (GWP) during the design life of pavements; and iii) study the effect of NGWBT market penetration, granular layer strength, and traffic level through the sensitivity analysis. In addition, 1.5% fuel saving per NGWBT axle was assumed, as it reasonably estimates the fuel economy improvement.

5.1 METHODOLOGY

The pavement LCA has five stages as defined in Figure 0-1. In this study, all stages, except end of life, are considered.

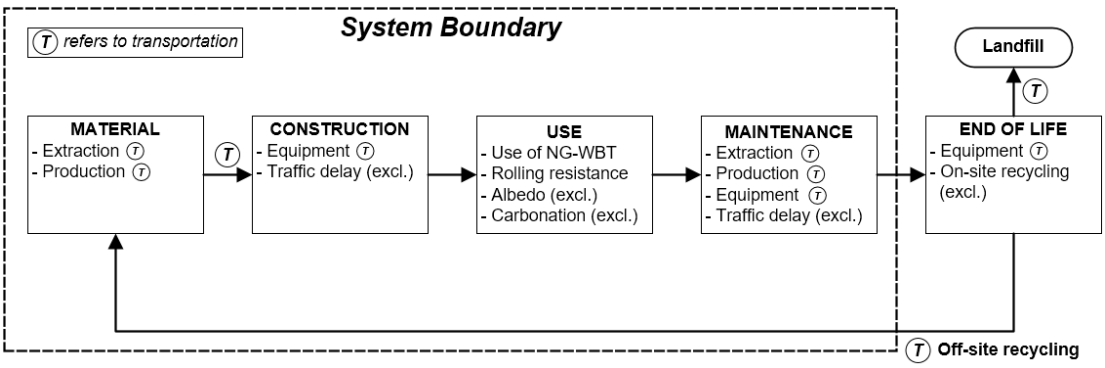

Figure 0-1. Generic life-cycle stages of pavement with defined system boundary.

The methodology suggested to conduct the LCA analysis is illustrated in Figure 0-2. Key variables in the study include the following:

- Tire type (DTA and NGWBT)
- NGWBT market penetration (0, 5, 10, 50, and 100%)
- Base/subbase stiffnesses (SS, WW, MM, MW, MS; where "S" refers to strong, "M" refers to medium, and "W" refers to weak)
- Seasonal stiffness of surface AC
- Traffic levels ("low" = AADT of 7,631 with a 20% truck, and "high" =AADT of 38,155 with a 20% truck)

Different pavement responses resulting from using DTA and NGWBT represent the starting point of the LCA study. Assuming all trucks are equipped with either DTA or NGWBT is insufficient to see how the environmental impacts change between the two cases, so five different levels (0, 5, 10, 50, and 100%) of NGWBT market penetration are used. As seen in previous chapters, the use of different base/subbase and seasonal AC stiffness can influence strain values at critical locations (bottom of HMA surface and top of subgrade) that may affect the result of the LCA analysis. In addition, two different traffic levels are considered to predict the expected life of pavements. All structural layers above the subgrade of a two-lane mainline pavement are considered in the study.

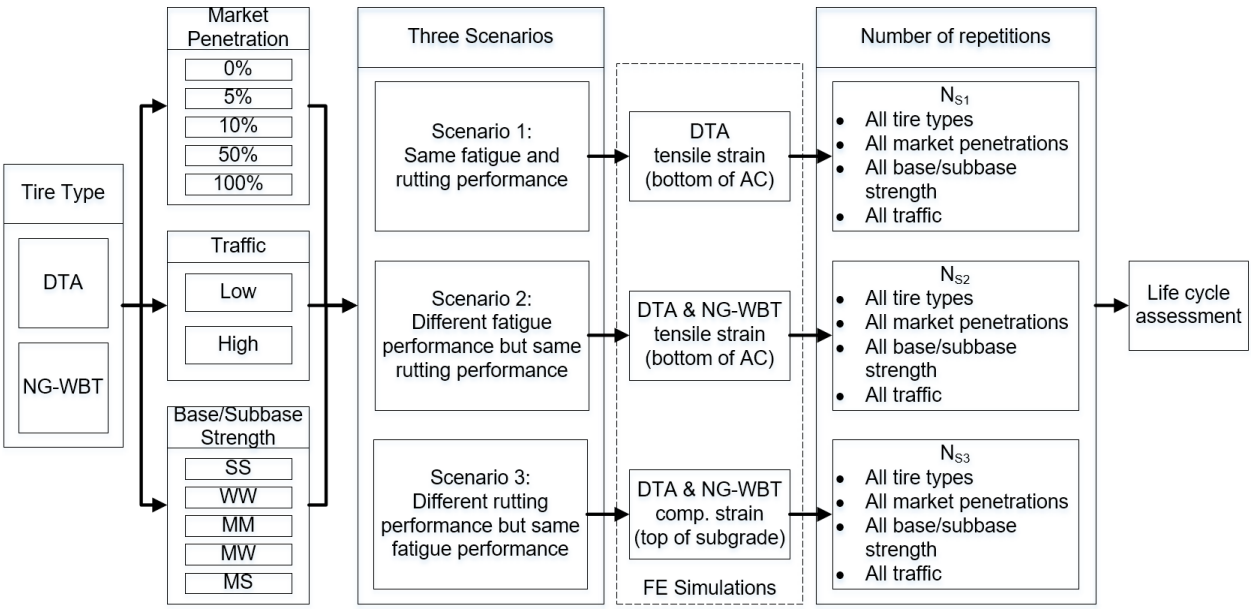

Figure 0-2. A general methodology for analyzing the impact of NGWBT.

Two environmental impacts—global warming potential (GWP) and energy consumption—are considered. Energy consumption refers to the primary and secondary energy consumed in material production and construction equipment operation but excludes the feedstock energy of asphalt binder. The embodied energy of fuel combusted is considered in the use phase. The analysis period of the study is 48 years and the functional unit is project-mile. U.S. Environmental Protection Agency (EPA) Tools for Reduction and Assessment of Chemicals and Other Environmental Impacts (TRACI) 2.1 was used for impact characterization.

For material and construction stages, life-cycle inventory (LCI) data are primarily adopted from commercial LCI database and literatures. Detailed information of AC mix design, material and construction, LCI data sources, and other material properties are listed in Appendix D. Traffic delays caused by construction activities are not considered assuming maintenance/rehabilitation take place at night time. A default maintenance schedule of pavements (Appendix D) is obtained from the IDOT manual (IDOT, 2013) but modified when needed to reflect the variations in pavement performance due to roughness, fatigue cracking, or rutting. In other words, a pavement rehabilitation is triggered when one of the following conditions is met:

- IRI is greater than or equal to 2.76 m/km (175 in/mi) – the IRI threshold value
- Cumulative traffic (ESAL) exceeds AC fatigue allowable repetitions
- Cumulative traffic (ESAL) exceeds subgrade rutting allowable repetitions

The allowable number of repetitions for fatigue and rutting is calculated based on the Asphalt Institute transfer functions (Appendix E). Rolling resistance induced by pavement roughness and fuel saving from NGWBT are considered in the use phase. Pavement roughness is quantified using International Roughness Index (IRI) and a use phase model is used to calculate the additional fuel consumption due to pavement roughness (Ziyadi et al., 2017b). As aforementioned, a 1.5% fuel saving per axle is considered for trucks equipped with NGWBT. The IRI progression is computed based on

the historical IRI data of a principal arterial highway in New Brunswick and has the following form:

$$IRI(t) = 1.0876e^{0.0607t} \quad (0\text{-}1)$$

Every time rehabilitation is applied, the IRI value drops to the initial IRI value, $IRI(t = 0)$, and progresses as predicted by Eq. (5.1). Since the IRI progression for NGWBT is not developed to date, the following three scenarios are assumed:

- Scenario 1: DTA and NGWBT have the same fatigue cracking and rutting potential; therefore, the only difference comes from the fuel saving from NGWBT
- Scenario 2: DTA and NGWBT have different fatigue cracking potential but the same rutting potential. The fuel saving from NGWBT still applies
- Scenario 3: DTA and NGWBT have the same fatigue cracking potential but different rutting potential. The rutting performance is used as an approximate indicator for roughness performance; and IRI performance between DTA and NGWBT is calculated using the equation below (Von Quintus et al., 2001). Examples of IRI progression for the low and high traffic levels and different levels of NGWBT market penetration are shown in Appendix F

$$\Delta IRI_{WBT_{year_j - year_i}} = \Delta IRI_{DTA_{year_j - year_i}} \times \frac{Rutting\ life\ with\ DTA}{Rutting\ life\ with\ WBT} \quad (0\text{-}2)$$

where: $\Delta IRI_{WBT_{year_j - year_i}}$ Increase in IRI value between year j and i under NGWBT (m/km)

$\Delta IRI_{DTA_{year_j - year_i}}$ Increase in IRI value between year j and i under DTA (m/km)

$Rutting\ life\ with\ DTA$ Pavement design life based on the rutting model under DTA

$Rutting\ life\ with\ WBT$ Pavement design life based on the rutting model under NGWBT.

To account for seasonal effects, an average annual damage value is used. For all scenarios, tire types, market penetrations, base–subbase strengths, and traffic levels

considered, the number of repetitions to failure is calculated; by dividing the cumulative traffic by the number of repetitions to failure, the annual damage value is calculated; and using Miner's Rule, pavement design life (until the next rehabilitation is triggered) is computed.

5.2 RESULTS AND DISCUSSION

The results of the LCA analysis are shown per the functional unit. The discussion is only limited to the case for the strong base and the strong subbase; results of other base/subbase cases are included in Appendix G. This section is based on 100% axle with NGWBT; an example result of 50% axle with NGWBT is shown in Appendix H. The negative value in the following figures means the environmental savings whereas the positive value refers to the burdens.

5.2.1 Scenario 1: Same Fatigue and Rutting Potential Between DTA And NGWBT

Figure 0-3 presents the energy consumption and GWP for Scenario 1. For both low and high traffic levels, rehabilitation is triggered by IRI. The environmental impacts in material, construction, and maintenance stages remain the same because DTA and NGWBT have the same fatigue and rutting performance, but the only saving in this scenario comes from the lower fuel consumption of NGWBT, as seen in Figure 0-3. The IRI progression used for the high traffic level is higher than that for the low traffic level, as seen in Appendix F.

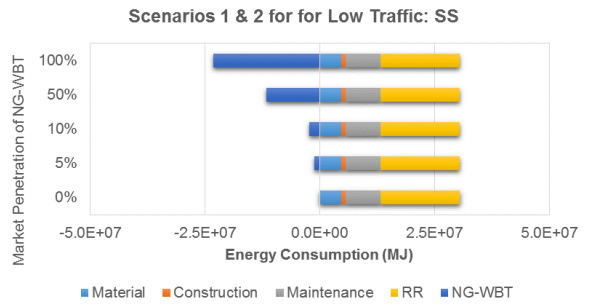

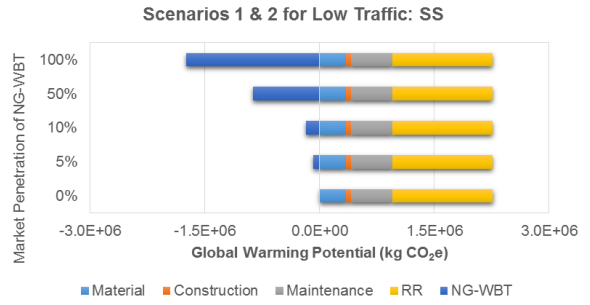

(a)

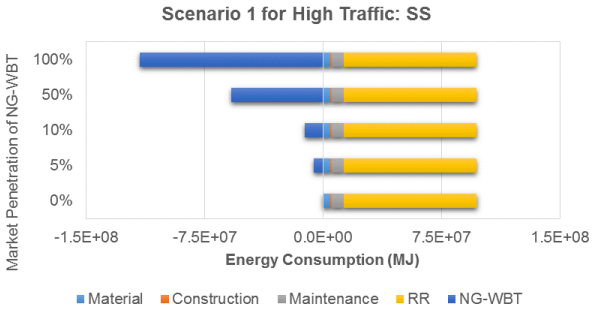

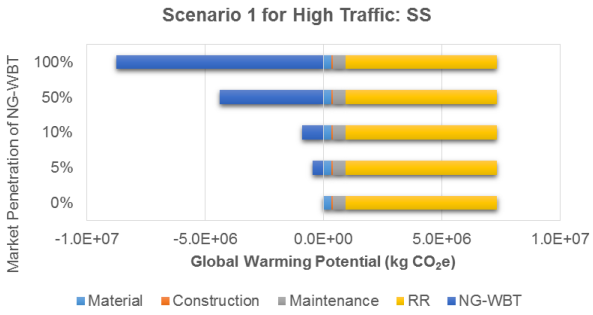

(b)

Figure 0-3. Energy consumption and GWP for Scenario 1 for (a) the low traffic level, and (b) the high traffic level (RR = rolling resistance induced by pavement roughness).

5.2.2 Scenario 2: Different Fatigue Cracking Potential but Same Rutting Potential

As presented in Figure 0-4, the two traffic levels show different results in Scenario 2. For the low traffic level, pavement rehabilitation is triggered by IRI because the time to reach the fatigue cracking failure is much longer than the IRI threshold. Therefore, the LCA result for the low traffic level is the same as in Scenario 1 (Figure 0-3). On the other hand, the design life of the pavement is primarily determined by the fatigue cracking potential for the high traffic level; therefore, the number of rehabilitation during the analysis period and pavement roughness progression are different for each market penetration of NGWBT. For example, for the 100% market penetration, more frequent rehabilitations cause increased environmental burdens in construction and maintenance stages, but reduced the impact from rolling resistance induced by roughness as presented in Figure 0-4.

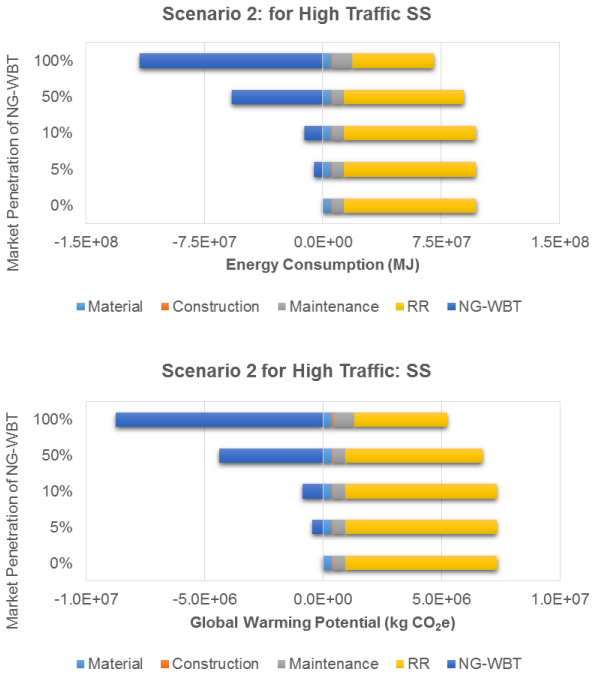

Figure 0-4. Energy consumption and GWP for Scenario 2 for the high traffic level.

5.2.3 Scenario 3: Same Fatigue Cracking Potential but Different Rutting Potential

In this scenario, IRI is changing with the market penetration of NGWBT because IRI is proportional to the rutting potential. In other words, NGWBT has a higher rutting potential than the DTA, so NGWBT has a faster IRI progression. However, the difference in IRI progression between DTA and NGWBT is not very significant; only the small amount of additional impacts is added to the result for the low traffic level as shown in Figure 0-5. For the high traffic level, rehabilitation takes place earlier in 100% market penetration so the impact from rolling resistance is relatively smaller than other market penetrations from a well-maintained pavement roughness as seen in Figure 0-5.

In summary, it is evident that the greater the NGWBT market penetration, the higher the fuel savings and, consequently, the fewer the emissions and greenhouse gases. However, this may vary depending on the scenario. Although in Scenario 2 more rehabilitation is expected due to increasing the NGWBT market penetration, smoother pavement is expected over the pavement life; this results in a reduced rolling resistance induced by roughness.

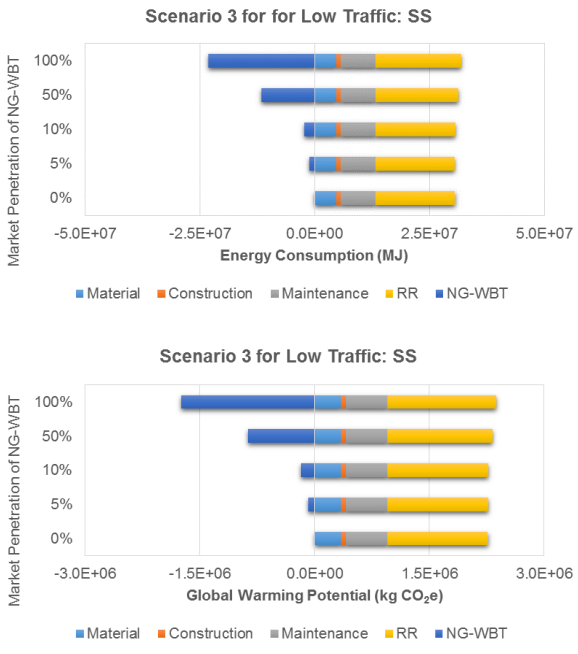

(a)

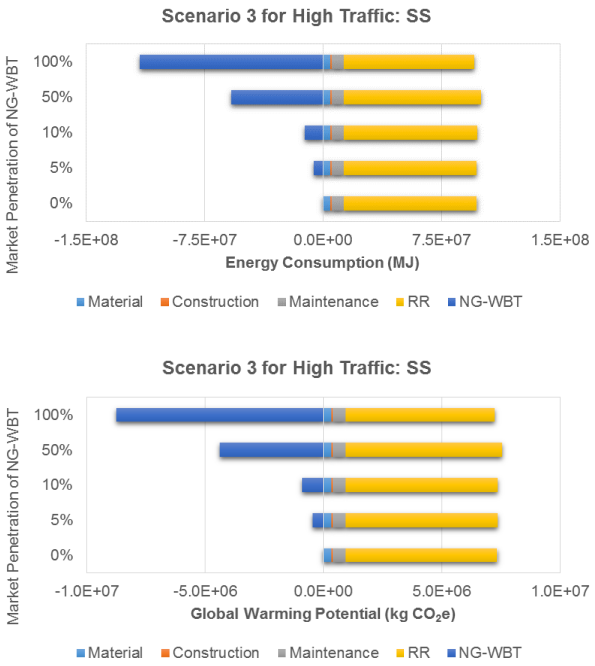

(b)

Figure 0-5. Energy consumption and GWP for Scenario 3 for (a) the low traffic level, and (b) the high traffic level.

CHAPTER 6:

PAVEMENT DAMAGE AND DESIGN TOOL

As part of the study, a user-friendly tool was developed using visual basic to help in the implementation of the findings of this research. The initial interface of the New Brunswick Pavement Analysis Tool (NBPAT) is presented in Figure 0-1. The names and usages of the tool subsections are as follow:

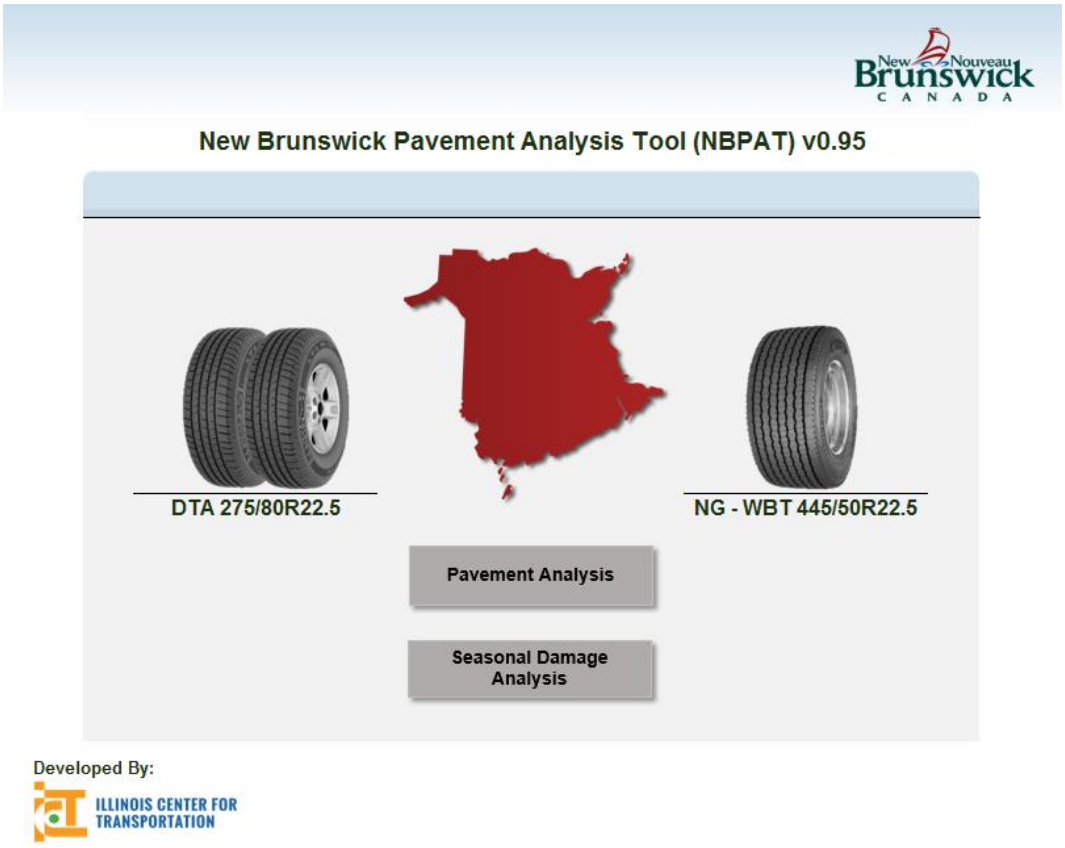

Figure 0-1. Tool interface.

6.1 NEW BRUNSWICK PAVEMENT DAMAGE SECTION (NBPDAS)

NBPDAS is a combined NGWBT to DTA damage ratio calculator. Based on the season, base and subbase modulus, this tool can predict the total number of repetitions to

failure for each of the four distresses considered in this study. In addition, the combined NGWBT to DTA damage ratio is also calculated. The inputs of this engine are the material properties of the base and subbase layer (MPa), and the season of interest (Fall, Winter, Spring or Summer). On the other hand, the outputs are the number of repetitions to failure for each tire configuration and pavement distress, and the combined NGWBT to DTA damage ratio.

6.2 NEW BRUNSWICK PAVEMENT EVALUATION SECTION (NBPEVS)

NBPDES is a tool used for evaluating pavement sections. By providing base and subbase material properties and traffic information, the user can check if the section is adequate for the predefined design life. This tool also helps in the optimization of base and subbase material selection since alternatives can be easily compared. Moreover, the effect of an increase market penetration and percentage of axles with NGWBT can be assessed. The inputs of this section are the material properties of base and subbase layer (MPa), design life (years), market penetration (%), percentage of trucks using NGWBT, percentage of axles with NGWBT (%) for the trucks using NGWBT; percentage trucks (%); truck factor; traffic growth rate (%); directional AADT; and lane distribution factor. The output is composed by a pass/fail check for the predefined design life with respect to the distresses considered.

CHAPTER 7:

SUMMARY

The impact of NGWBT and DTA on a representative pavement section of New Brunswick, Canada, was studied using finite element method (FEM) analysis and life-cycle assessment (LCA). The finite element analysis included features representing material behavior and loading, usually overlooked in the conventional analysis of flexible pavement; the procedure adopted for its development has been validated with experimental measurements. In particular, loading assumption are particularly important when comparing NGWBT and DTA because the distribution of tire–pavement contact stresses is very different for each tire. Regarding environmental impact, global warming potential and energy consumption were obtained from the life-cycle assessment (LCA) in three scenarios depending on the cracking and rutting potential due to the loading by each tire.

Based on the results of both analysis, the following conclusions can be drawn:

- In general, NGWBT created greater critical pavement responses. The highest difference was seen on the near-surface responses (i.e., maximum shear strain in the AC). The difference between both tires became negligible for the maximum vertical strain on top of the subgrade, which is responsible for secondary rutting. The use of high quality and durable AC may minimize this impact.
- Under realistic setting, it was found that pavement damage increased with NGWBT market penetration. For example, a market penetration of around 20% NGWBT can cause an increment of 8% in pavement damage for the cases studied. It has to be noted that traffic on the pavement studied is considered very low and hence the possible extra damage related to NGWBT could possibly be handled by the pavement structure.

- Savings in global warming potential and energy consumption due to NGWBT usage depended on market penetration (higher NGWBT market penetration resulted in higher environmental benefits; but possibly greater pavement damage).
- Steering wheel impact was not considered in this study and is expected to have significant impact on the pavement response. Hence, it is recommended that a full truck analysis be analyzed in the future.

REFERENCES

Al-Qadi, I. L., Elseifi, M. A., Yoo, P. J. (2004). Pavement Damage due to Different Tires and Vehicle Configurations, Virginia Tech Transportation Institute, Blacksburg, Virginia.

Al-Qadi, I. L., Elseifi, M. A., Yoo, P. J., Janajreh, I. (2005a). "Pavement Damage due to Conventional and New Generation of Wide-Base Super Single Tires." *Tire Science and Technology*, 33(4), 210-226.

Al-Qadi, I. L., and Elseifi, M. A. (2008). New Generation of Wide-Base Tires: Impact on Trucking Operations, Environment, and Pavements. In Transportation Research Record: Journal of the Transportation Research Board, No. 1981, Transportation Research Board of the National Academies, Washington, D.C., 2008, pp. 100 – 109

Al-Qadi, I. L., Yoo, P. J., Elseifi, M. A., Janajreh, I. (2005b). "Effects of Tire Configurations on Pavement Damage." *Journal of the Association of Asphalt Paving Technologists*, 84, 921-962.

Al-Qadi, I. L., and Yoo, P. J. (2007). Effect of Surface Tangential Contact Stresses on Flexible Pavement Response (With Discussion). *Journal of the Association of Asphalt Paving Technologists*, 76.

Al-Qadi, I. L., and Wang, H. (2009a). "Full-Depth Pavement Responses Under various Tire Configurations: Accelerated Pavement Testing and Finite Element Modeling." *Journal of the Association of Asphalt Paving Technologists*, 78, 645-680.

Al-Qadi, I. L., and Wang, H. (2009b). Evaluation of Pavement Damage due to New Tire Design, Illinois Center for Transportation, Rantoul, IL.

Al-Qadi, I. L., and Wang, H. (2009c). Pavement Damage due to Different Tire and Loading Configurations on Secondary Roads, NEXTRANS University Transportation Center, West Lafayette, Indiana.

Al-Qadi, I. L., Wang, H., Tutumluer, E. (2010). "Dynamic Analysis of Thin Asphalt Pavement by using Cross-Anisotropic Stress-Dependent Properties for Granular Layer." *Transportation Research Record: Journal of the Transportation Research Board*, 2154, 156-163.

Ang-Olson, J., & Schroeer, W. (2002). Energy Efficiency Strategies for Freight Trucking: Potential Impact on Fuel use and Greenhouse Gas Emissions. T*ransportation Research Record: Journal of the Transportation Research Board*, (1815), 11-18.

Bare, J. (2012). Tool for the Reduction and Assessment of Chemical and Other Environmental Impacts (TRACI, Version 2.1). [Software]. U.S. Environmental Protection Agency, Cincinnati, OH.

Bonaquist, R. (1992). An Assessment of the Increased Damage Potential of Wide Base Single Tires. 7th International Conference on Asphalt Pavements, Nottingham, UK, pp. 1-16.

COST 334. (2001). "Effects of Wide Single Tires and Dual Tires, Final Report of the Action" European Cooperation in the Field of Scientific and Technical Research, Brussels, Belgium.

De Beer, M., & Fisher, C. (2013). Stress-In-Motion (SIM) system for capturing tri-axial tyre–road interaction in the contact patch. *Measurement*, *46*(7), 2155-2173.

Dessouky, S. H., Al-Qadi, I. L., & Yoo, P. J. (2014). Full-depth flexible pavement responses to different truck tyre geometry configurations. *International Journal of Pavement Engineering*, *15*(6), 512-520.

EarthShift (2013). US-Ecoinvent Database. Version 2.2. [Database]. Swiss Center for Life-Cycle Inventories, St-Gallen, Switzerland.

Elseifi, M. A., Al-Qadi, I. L., Yoo, P. J. (2006). "Viscoelastic Modeling and Field Validation of Flexible Pavements." *Journal of Engineering Mechanics*, 132(2), 172-178.

Environment and Climate Change Canada (2016). Canadian Environmental Sustainability Indicators: Greenhouse Gas Emissions. Retrieved from www.ec.gc.ca/indicateurs-indicators/default.asp?lang=en&n=FBF8455E-1.

Franzese, O., Knee, H. E., and Slezak, L. (2010). Effect of Wide-Based Single Tires on Fuel Efficiency of Class 8 Combination Trucks. Transportation Research Record, No. 2191, pp. 1-7.

GENIVAR Consulting Group (2005). "Economic Study Use of Supersingle Tires by Heavy Vehicles Operating in Québec." Report published by GENIVAR Consulting Group, Montreal, QC, Canada.

Gillespie, T. D., Karamihas, S. M., Sayers, M. W., Nasim, M. A., Hansen, W., Ehsan, N., Cebon, D. (1992). Effect of Heavy-Vehicle Characteristics on Pavement Response and Performance, Transportation Research Board, Washington, D.C.

Greene, J., Toros, U., Kim, S., Byron, T., Choubane, B. (2009). Impact of Wide-Base Single Tires on Pavement Damage, Florida Department of Transportation.

Grellet, D., Doré, G., & Bilodeau, J. P. (2012). Comparative Study on the Impact of Wide Base Tires and Dual Tires on the Strains Occurring Within Flexible Pavements Asphalt Concrete Surface Course. *Canadian Journal of Civil Engineering*, 39(5), 526-535.

Grellet, D., Doré, G., Bilodeau, J. P., & Gauliard, T. (2013). Wide-Base Single-Tire and Dual-Tire Assemblies: Comparison Based on Experimental Pavement Response and Predicted Damage. *Transportation Research Record: Journal of the Transportation Research Board*, (2369), 47-56.

Gungor, O. E., Al-Qadi, I. L., Gamez, A., & Hernandez, J. A. (2016). In-Situ Validation of Three-Dimensional Pavement Finite Element Models. In *The Roles of Accelerated Pavement Testing in Pavement Sustainability* (pp. 145-159). Springer International Publishing.

Harvey, J. T., & Popescu, L. (2000). Rutting of Caltrans Asphalt Concrete and Asphalt-Rubber Hot Mix under Different Wheels, Tire and Temperature-Accelerated Pavement Testing Evaluation. *Berkeley: Pavement Research Center, Institute of Transportation Studies, University of California*.

Harvey, J., Meijer, J., Ozer, H., Al-Qadi, I. L., Saboori, A., and A. Kendall. (2016). Pavement Life-Cycle Assessment Framework. FHWA-HIF-16-014. Federal Highway Administration, Washington, D.C.

Häkkinen, T., & Mäkelä, K. (1996). Environmental Adaption of Concrete. Environmental Impact of Concrete and Asphalt Pavements. Research Notes 1752. Technical Research Centre of Finland.

Hernandez, J. A., Al-Qadi, I., & De Beer, M. (2013). Impact of Tire Loading and Tire Pressure on Measured 3-D Contact Stresses. In *Airfield and highway pavement 2013: Sustainable and efficient pavements* (pp. 551-560).

Hernandez, J. A., Gamez, A., & Al-Qadi, I. L. (2016). Effect of Wide-Base Tires on Nationwide Flexible Pavement Systems: Numerical modeling. *Transportation Research Record: Journal of the Transportation Research Board*, (2590), 104-112.

Huhtala, M., Pihlajamaki, J., & Pienimaki, M. (1989). Effects of Tires and Tire Pressures on Road Pavements. *Transportation research record*, *1227*, 107-114.

Huhtala, M. (1986, June). The Effect of Different Trucks on Road Pavements. In *International Symposium on Heavy Vehicle Weights and Dimensions, Kelowna, British Columbia, Proceedings* (pp. 151-9).

Illinois Department of Transportation (2013). Chapter Fifty-four Pavement Design. Bureau of Design and Environment Manual. Springfield, IL.

Kang, S., Al-Qadi, I. L., Ozer, H., Ziyadi, M., and Harvey, J. (2017). Environmental and Economic Impact of Using New Generation Wide-Base Tires*. Transportation Research Part D: Transport and Environment* (submitted).

Kim, D., Salgado, R., Altschaeffl, E. G. (2005). "Effects of Super-Single Tire Loadings on Pavements." *Journal of Transportation Engineering*, 131(10), 732-743.

Kim, Minkwan, Erol Tutumluer, and Jayhyun Kwon. (2009). "Nonlinear Pavement Foundation Modeling for Three-Dimensional Finite-Element Analysis of Flexible Pavements." *International Journal of Geomechanics.*

Michelin (2016). Choose Michelin X One Tires. Retrieved from https://www.michelinb2b.com/wps/b2bcontent/PDF/MICHELIN_X_One_Brocue.pdf

Perdomo, D., and Nokes, B. (1993). Theoretical Analysis of the Effects of Wide-Base Tires on Flexible Pavements using CIRCLY. *Transportation Research Record: Journal of the Transportation Research Board*, 1388, 108-119.

Pierre, P., Dore, G., Vagile, L. (2003). Characterization and Evaluation of Tire-Roadway Interface Stresses, Ministry of Transport, University of Laval, Quebec, Canada.

Priest, A. L., and Timm, D. H. (2006). "Mechanistic Comparison of Wide-Base Single versus Standard Dual Tire Configurations." *Transportation Research Record: Journal of the Transportation Research Board*, 1949(155), 163.

Ponniah, J., Madill, R., Marchand, S., Corredor, A., Haas, R., and Lane, B. (2010). Challenges in Decreasing Greenhouse Gas Emissions by Increasing the Axle Load Permitted on Wide Base Single Tires. Annual Conference of the Transportation Association of Canada, Halifax, Nova Scotia, Canada.

Santero, N. (2009). Pavements and the Environment: A Life-Cycle Assessment Approach. Ph.D. Thesis. Department of Civil and Environmental Engineering, University of California, Berkeley.

Sebaaly, P. E., and Tabatabaee, N. (1989). Effect of Tire Pressure and Type on Response of Flexible Pavement. *Transportation Research Record: Journal of the Transportation Research Board*, 1227, 115-127.

Sebaaly, P. E., & Tabatabaee, N. (1992). Effect of Tire Parameters on Pavement Damage and Load-Equivalency Factors. *Journal of transportation engineering*, *118*(6), 805-819.

Siddharthan, R. V., Krishnamenon, N., El-Mously, M., Sebaaly, P. E. (2002). Investigation of Tire Contact Stress Distributions on Pavement Response. *Journal of Transportation Engineering*, 128(2), 136-144.

Stripple, H. (2001). Life cycle analysis of road; A pilot Study for Inventory Analysis, Swedish Environmental Research Institute (IVL), Gothenburg, Sweden.

Tutumluer, E. (2008). State of the Art: Anisotropic Characterization of Unbound Aggregate Layers in Flexible Pavements. Engineering Mechanics Conference. Minneapolis, MN.

Tutumluer, E. and Thompson, M. (1998). Anisotropic Modeling of Granular Bases. Final Report for the Federal Highway Administration.

U.S. Environmental Protection Agency (EPA). SmartWay: Low Rolling Resistance Tires (Report No. EPA-420-F-16-024). Retrieved from https://www.epa.gov/sites/production/files/2016- 06/documents/420f16024.pdf

U.S. Environmental Protection Agency (2015). Motor Vehicle Emission Simulator (MOVES) 2014a. [Software]. Washington, D.C.

Van Dam, T., Harvey, J., Muench, S., Smith, K., Snyder, M., Al-Qadi, I., Ozer, H., Meijer, J., Ram., R. V., Roesler, J. R., and A. Kendall. (2015). Towards Sustainable Pavement Systems: A Reference Document. FHWA-HIF-15-002. Federal Highway Administration. Washington D.C.

Von Quintus, H. L., Yau, A., Witczak, M. W., Andrei, D., and Houston, W. N. (2001). Appendix OO-1: Background and Preliminary Smoothness Prediction Models for Flexible Pavements. Guide for Mechanistic-Empirical Design of New and Rehabilitated Pavement Structures. Final Report NCHRP 1-37A Project. Transportation Research Board, Washington, D.C.

Wang, D., Roesler, J. R., & Guo, D. Z. (2009). Analytical Approach to Predicting Temperature Fields in Multilayered Pavement Systems. *Journal of Engineering Mechanics*, 135(4), 334-344.

Wang, T., Lee, I. -., Kendall, A., Harvey, J., Lee, E. -., & Kim, C. (2012). Life Cycle Energy Consumption and GHG Emission from Pavement Rehabilitation with Different Rolling Resistance. Journal of Cleaner Production, 33, 86-96. doi:10.1016/j.jclepro.2012.05.001

Wirtgen. (n.d.). Brochure for DV+ 90i VO-S roller. Retrieved from http://www.hamm.eu/en/products/tandem-rollers/series-dv/dv-90i-vo-s.185425.php

Wirtgen. (n.d.). Brochure for Super 1303-3 paver. Retrieved from http://www.voegele.info/en/products/super-series/compact-class/super-1303-3/highlights.php

Wirtgen. (n.d.). Brochure for W220 Milling Machine. Retrieved from http://www.wirtgen.de/en/products/cold-milling-machines/large-milling-machines/w220.php

WSP Canada (2015). "New Generation Wide Base Single (NGWBS) Tires Study Cost-Benefit Analysis of the Removal of the Weight Limitation for NGWBS Tires Final Report." Report published by WSP Canada, Quebec, QC, Canada.

Xue, W., & Weaver, E. (2015). Influence of Tyre Configuration on Pavement Response and Predicted Distress. International Journal of Pavement Engineering, 16(6), 538-548.

Yoo, P. J., Al-Qadi, I. L., Elseifi, M. A., & Janajreh, I. (2006). Flexible pavement responses to different loading amplitudes considering layer interface condition and lateral shear forces. *The International Journal of Pavement Engineering*, *7*(1), 73-86.

Yoo, P., & Al-Qadi, I. (2007). Effect of transient dynamic loading on flexible pavements. *Transportation Research Record: Journal of the Transportation Research Board*, (1990), 129-140.

Yoo, P. J., and I. L. Al-Qadi. (2008) The Truth and Myth of Fatigue Cracking Potential in Hot-Mix Asphalt: Numerical Analysis and Validation. Journal of Association of Asphalt Paving Technologists, 77, 549–590.

Yoo, P. J., Al-Qadi, I. L., Elseifi, M. A., and Janajreh, I. (2006). Flexible Pavement Responses to Different Loading Amplitudes Considering Layer Interface Condition and Lateral Shear Forces. The International Journal of Pavement Engineering, 7(1), 73-86.

Ziyadi, M., Ozer, H., and Al-Qadi, I, L. (2017a). Quantitative Assessment of the Use Phase Impact on a Comparative Pavement LCA. Transportation Research Board, Washington, D.C.

Ziyadi, M., Ozer, H., Kang, S., & Al-Qadi, I, L. (2017b). Pavement Roughness-Related Vehicle Energy Consumption and an Environmental Impact Calculation Model for Transportation Sector. Journal of Cleaner Production (submitted).

APPENDIX A:

CRITICAL PAVEMENT RESPONSES

SECTION: WEAK BASE AND SUBBASE

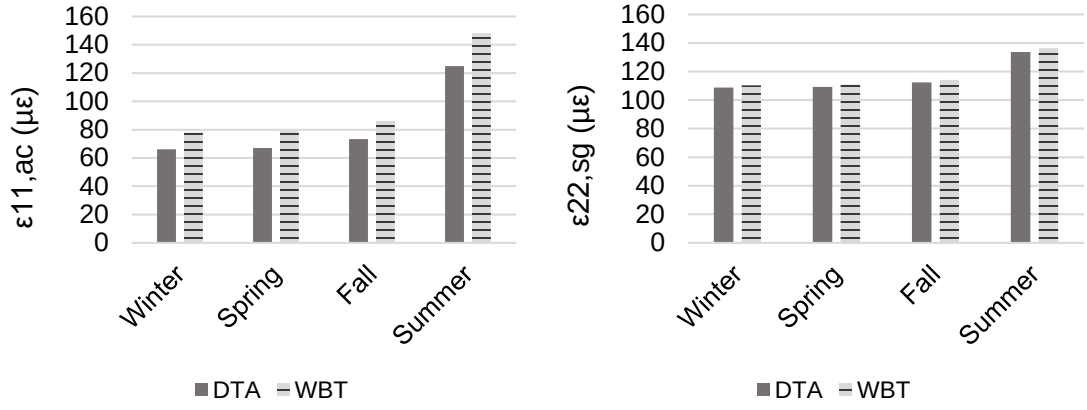

Figure A- 1. Tensile strain at the bottom of AC (left) and vertical strain on top of SG (right).

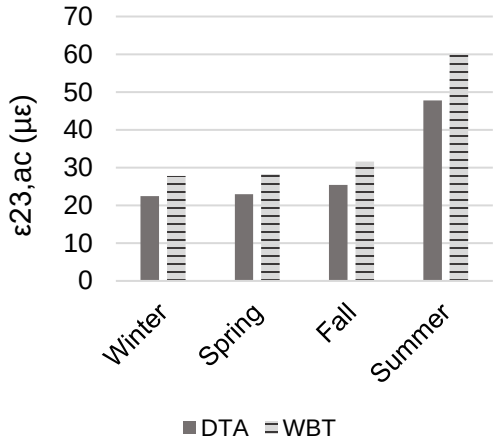

Figure A- 2. Shear strain within AC layer.

SECTION: MEDIUM BASE AND SUBBASE

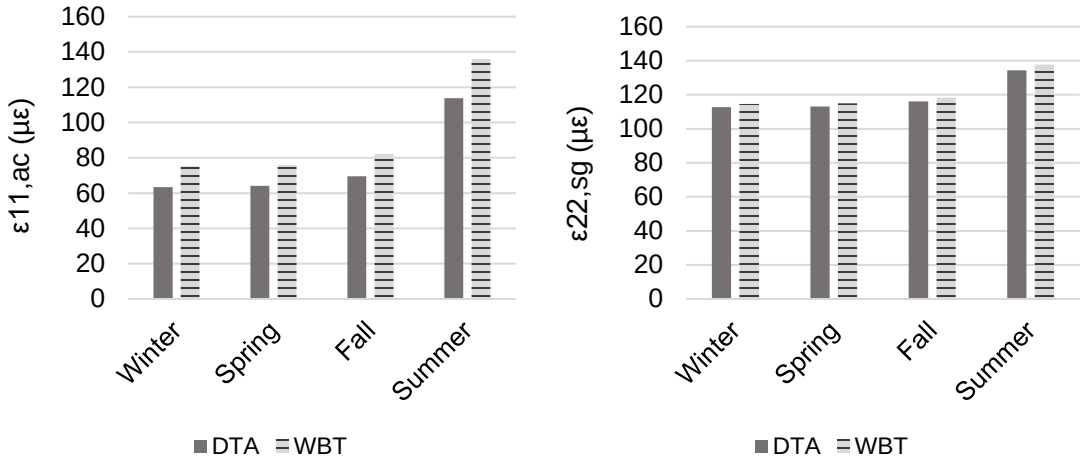

Figure A- 3. Tensile strain at the bottom of AC (left) and vertical strain on top of SG (right).

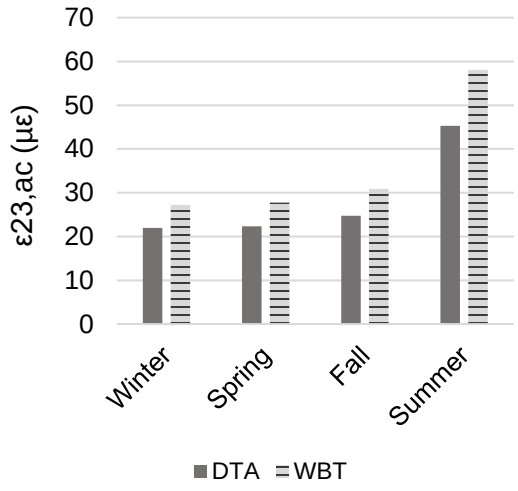

Figure A- 4. Shear strain within AC layer.

SECTION: MEDIUM BASE AND WEAK SUBBASE

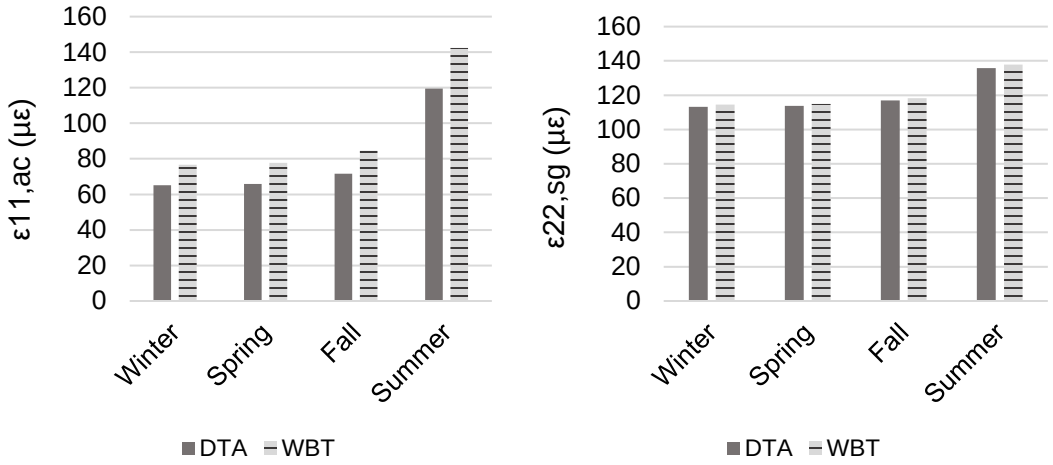

Figure A- 5. Tensile strain at the bottom of AC (left) and vertical strain on top of SG (right).

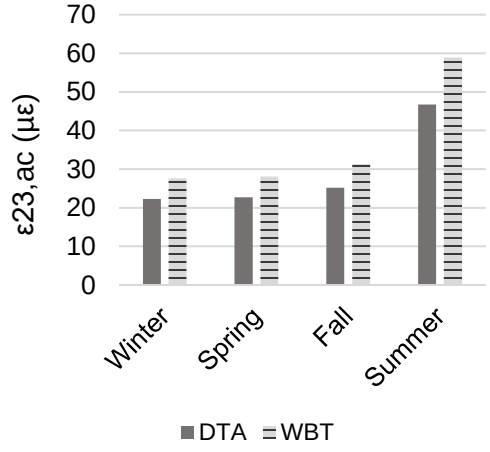

Figure A- 6. Shear strain within AC layer.

SECTION: MEDIUM BASE AND STRONG SUBBASE

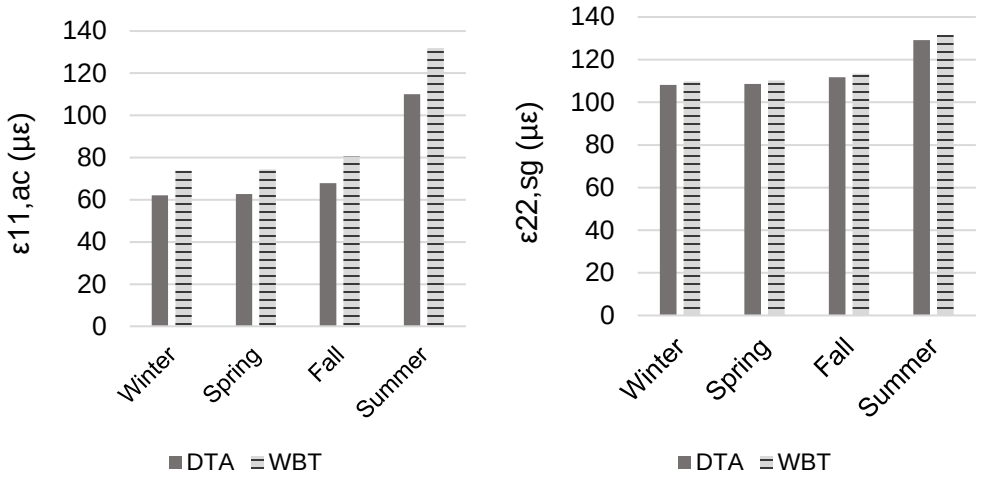

Figure A- 7. Tensile strain at the bottom of AC (left) and vertical strain on top of SG (right).

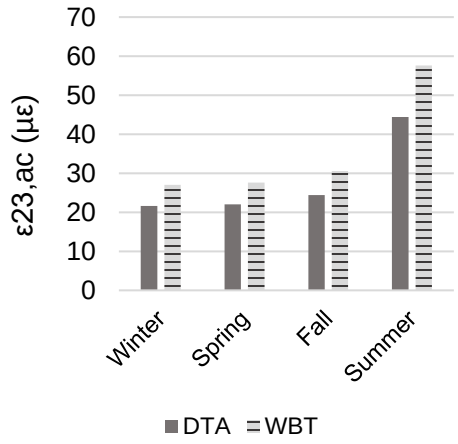

Figure A- 8. Shear strain within AC layer.

APPENDIX B:

TRANSFER FUNCTIONS

FATIGUE CRACKING

Number of repetitions to failure for the considered distresses was calculated using transfer functions implemented in MEPDG. The general equation to calculate fatigue cracking, either bottom-up or near-surface, is given by:

$$N_f = k_{f1} \times C \times C_H \times \beta_{f1}(\varepsilon_t)^{k_{f2}\beta_{f2}}(E)^{k_{f3}\beta_{f3}} \quad \text{(B-1)}$$

where $k_{f1,f2,f3}$ are global field calibration parameters (NCHRP 1-40D), ε_t is the tensile strain, k_{f1}= 0.007566, k_{f2}= -3.9492, k_{f3}= -1.281, $\beta_{f1,f2,f3}$ are local or field-mixture calibration constants (for global calibration, assume all to be 1.0), $C = 10^M$, and:

$$M = 4.84\left(\frac{V_b}{V_a + V_b} - 0.69\right) \quad \text{(B-2)}$$

where V_b is the effective binder content (%) and V_a is the air voids (%). The parameter C_H is Eq. (B-1) depends on the type of fatigue being studied:

$$C_H(bottom\ up) = \frac{1}{0.000398 + \frac{0.003602}{1 + e^{(11.02 - 3.49H_{HMA})}}} \quad \text{(B-3)}$$

$$C_H(near\ surface) = \frac{1}{0.01 + \frac{12.00}{1 + e^{(15.676 - 2.816H_{HMA})}}} \quad \text{(B-4)}$$

where H_{HMA} is the AC thickness. Additionally, the tensile strain in Eq. (B-1) is defined by the specific type of fatigue cracking studied: tensile strain at the bottom of the AC for bottom-up fatigue cracking, and shear strain for near-surface fatigue cracking.

AC RUTTING

The allowable number of load applications needed for HMA rutting failure can be calculated using the following equation:

$$\Delta_{p(HMA)} = \varepsilon_{p(HMA)} h_{HMA} = \beta_{1r} k_z \varepsilon_{r(HMA)} 10^{k_{1r}} n^{k_{2r},\beta_{2r}} T^{k_{3r},\beta_{3r}} \quad \text{(B-5)}$$

where $\Delta_{p(HMA)}$ is the accumulated permanent or plastic vertical deformation in the AC layer/sublayer in inches; $\varepsilon_{p(HMA)}$ is the accumulated permanent or plastic axial strain in the AC layer/sublayer; $\varepsilon_{r(HMA)}$ is the resilient or elastic strain calculated by the structural response model at the mid-depth of each HMA sublayer, in/in; h_{HMA} is the thickness of the AC layer/sublayer, in inches; n is the number of axle load repetitions, T is the pavement temperature in Fahrenheit degrees; k_z is the depth confinement factor; $k_{1r,2r,3r}$ are global field calibration parameters (from the NCHRP 1-40D recalibration); k_{1r}= -3.35412, k_{2r} = 0.4791, k_{3r} = 1.5606); $\beta_{1r,2r,3r}$ are local or mixture field calibration constants; for the global calibration, these constants were all set to 1.0. At the same time:

$$k_z = (C_1 + C_2 D) 0.328196^D \quad \text{(B-6)}$$

$$C_1 = -0.1039(h_{HMA})^2 + 2.4868 h_{HMA} - 17.342 \quad \text{(B-7)}$$

$$C_2 = -0.0172(h_{HMA})^2 - 1.7331 h_{HMA} + 27.428 \quad \text{(B-8)}$$

where D is the depth below the surface in inches.

SUBGRADE RUTTING

According to MEPDG, the total number of repetition to failure to create subgrade rutting failure is calculated as follows:

$$N_r = 1.365 \times 10^{-9} (\varepsilon_v)^{-4.477} \quad \text{(B-9)}$$

where N_r is the allowable number of axle load repetitions for subgrade rutting failure and ε_v is the maximum vertical strain on top of subgrade.

APPENDIX C:

DAMAGE RATIOS

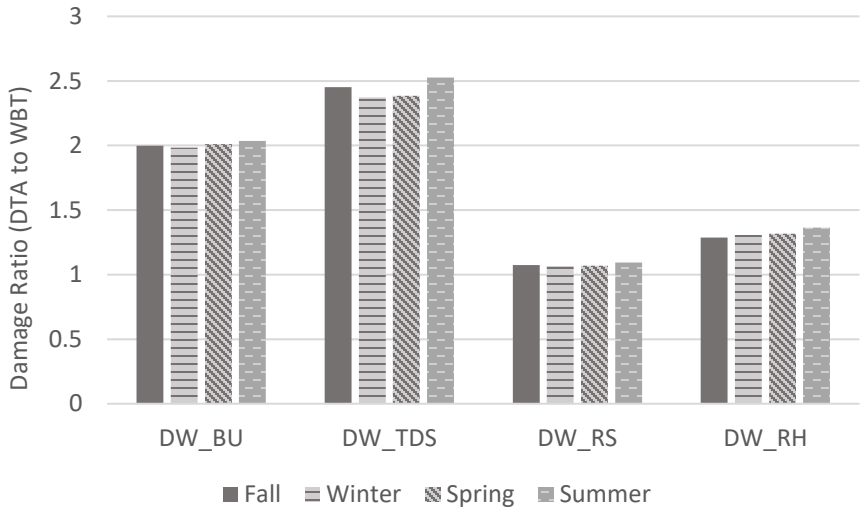

Figure C- 1 Damage ratio for considered distresses, seasons, and weak base and subbase.

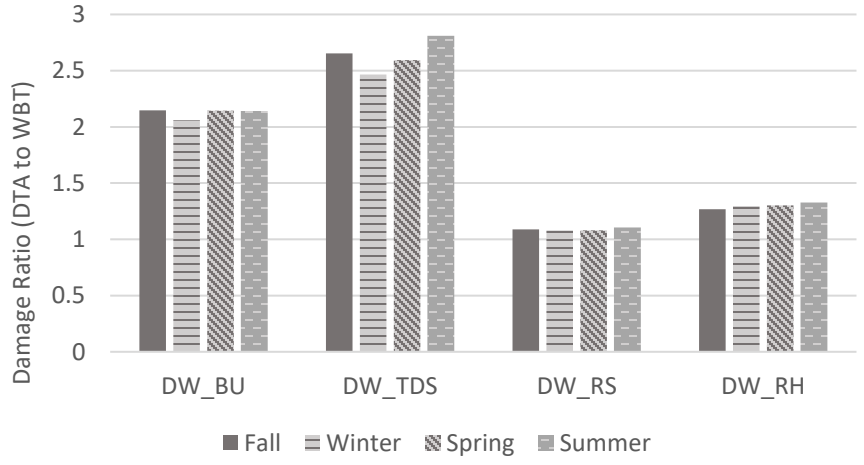

Figure C- 2. Damage ratio for considered distresses, seasons, and medium base and subbase.

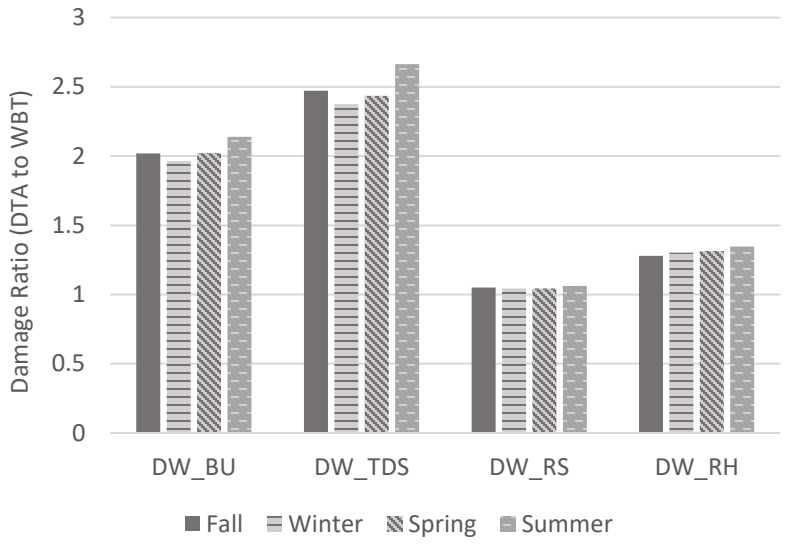

Figure C- 3. Damage ratio for considered distresses, seasons, and medium base and weak subbase.

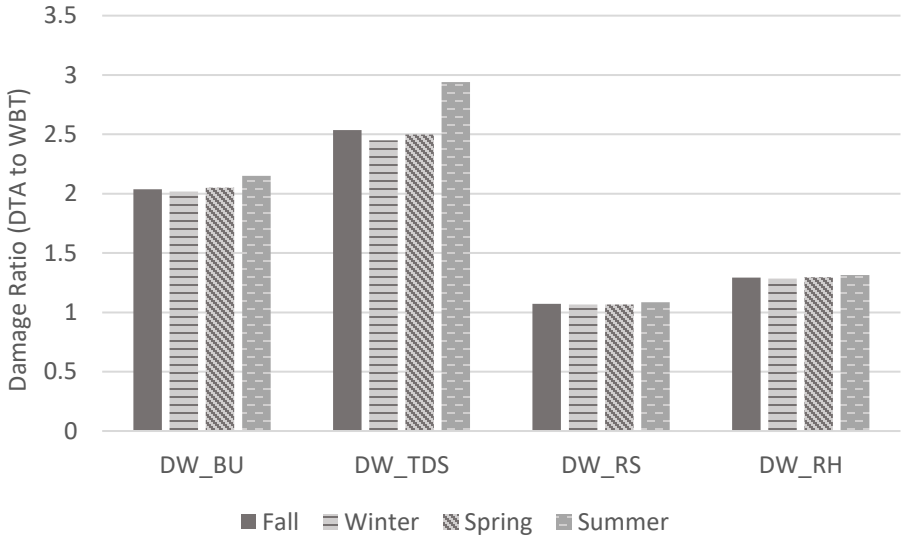

Figure C- 4. Damage ratio for considered distresses, seasons, and medium base and strong subbase.

APPENDIX D:

LCI INFORMATION FOR MATERIAL AND CONSTRUCTION STAGES

Table D- 1. Data Sources for Material and Construction Stages

Material	**Sources**	**Remark**
Straight binder	Meli (2006)	
Crushed rock	Earthshift (2013)	US-Ecoinvent 2.2; Limestone, crushed, for mill/US* US-EI U
Crushed gravel	Earthshift (2013)	US-Ecoinvent 2.2; Gravel, crushed, at mine/US* US-EI U
Fine aggregate	Meli (2006)	
Hauling	US EPA MOVES 2014a	
Reclaimed asphalt pavement (RAP)	Meli (2006)	
HMA plant	Meli (2006)	
Equipment	**Sources**	**Remark**
Paver	Vogele, US-Ecoinvent 2.2	Super 1303-3
Roller	Hamm, US-Ecoinvent 2.2	DV+ 90i VO-S
Milling machine	Wirtgen, US-Ecoinvent 2.2	W220

Table D- 2. AC Mix Design Information

Material	Recycled Asphalt Content (%)	Amount (% Mix)
Crushed stone	0.0	47.7
Crushed gravel	0.0	32.0
Fine aggregate	0.0	5.3
Recycled asphalt pavement	6.0	15.0
Straight binder	0.0	5.6

Table D- 3. Mix Design Volumetrics

Gmb (g/cm^3)	2.527
Gmm (g/cm^3)	2.619
Voids (%)	3.5
Asphalt content (%)	6.0

Table D- 4. Specific Gravity and Modulus of Granular Materials

Granular Materials	Specific Gravity	Modulus (MPa)
Crushed rock	2.815	132
Crushed gravel	2.815	132
Glacial till	2.72	56

Material	Description	Amount (% mix)
Crushed stone	CS	47.7
Crushed gravel	CG	32
Fine aggregate	FA	5.3

Mineral filler	MF	0
Default Recycled Asphalt Pavement	CAT 1 FINE	15
Straight binder	PG76-22	5.6

Table D- 5. Baseline Pavement Rehabilitation Schedule for High Traffic Level (Analysis Period: 48 Years)

Year	Mainline activity
2014	Reconstruction
2028	2.0 in (5.0 cm) mill and overlay & 2.0% partial depth patching
2042	2.0 in (5.0 cm) mill and 2.25 in (5.7 cm) overlay & 2.0% partial depth patching
2056	2.0 in (5.0 cm) mill and 2.25 in (5.7 cm) overlay & 2.0% partial depth patching

Table D- 6. Baseline Pavement Rehabilitation Schedule for Low Traffic Level (Analysis Period: 48 Years)

Year	Mainline activity
2014	Reconstruction
2030	2.0 in (5.0 cm) mill and overlay & 2.0% partial depth patching
2046	2.0 in (5.0 cm) mill and 2.25 in (5.7 cm) overlay & 2.0% partial depth patching

APPENDIX E:

ASPHALT INSTITUTE TRANSFER FUNCTIONS

Transfer functions from the Asphalt Institute (AI) were used to compute the number of repetition for each failure criteria. The result of using MEPDG transfer functions is used primarily for fatigue cracking progression so the AI transfer functions were used to determine the number of repetitions to failure in this study.

Bottom-up fatigue cracking

$$N_f = 0.0795 \times C\varepsilon_t^{-3.291}|E^*|^{-0.854} \quad \text{(E-1)}$$

$$C = 10^{4.84\left(\frac{V_b}{V_a+V_b}-0.69\right)} \quad \text{(E-2)}$$

where: N_f: maximum allowed repetition

C: correction factor

V_a: volume of asphalt in the mix

V_b: volume of air in the mix

ε_t: tensile strain; and

$|E^*|$: stiffness (dynamic modulus) of asphalt in units of psi.

Subgrade rutting

$$N_d = 1.365 \times 10^{-9}(\varepsilon_c)^{-4.447} \quad \text{(E-3)}$$

where: N_d: maximum number of axle loads to the rut depth failure criteria (0.5-in rut depth)

ε_c: vertical compressive strain on top of the subgrade

APPENDIX F:

ROUGHNESS PROGRESSION

Only one case for different traffic level and another for market penetration are shown here because other base–subbase combinations show more or less the same trend in the IRI progression. “SS” refers to strong base and strong subbase in the following figures.

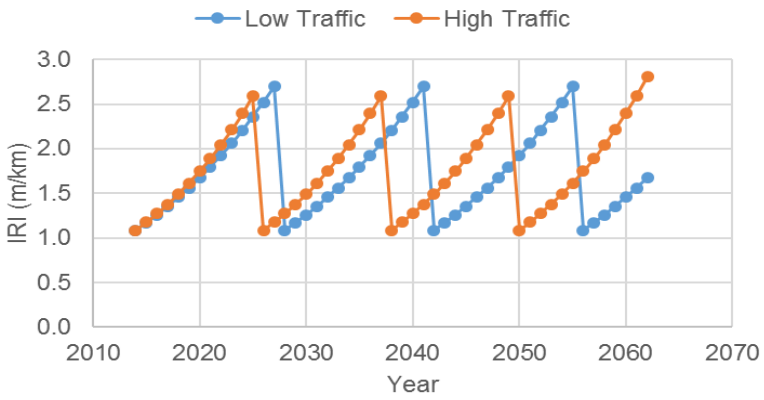

Figure F- 1. Comparison of IRI progression for high and low traffic levels based on Scenario 3 SS (Starting Year = 2014).

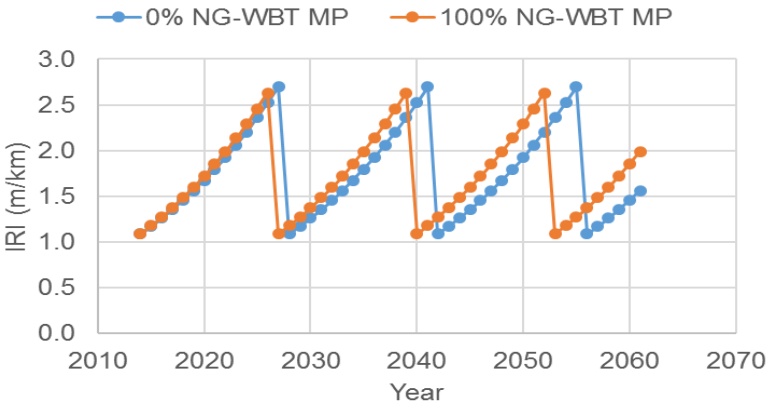

Figure F- 2. Progression of IRI progression for 0% and 100% NGWBT market penetration based on Scenario 3 SS and the high traffic level (Starting Year = 2014).

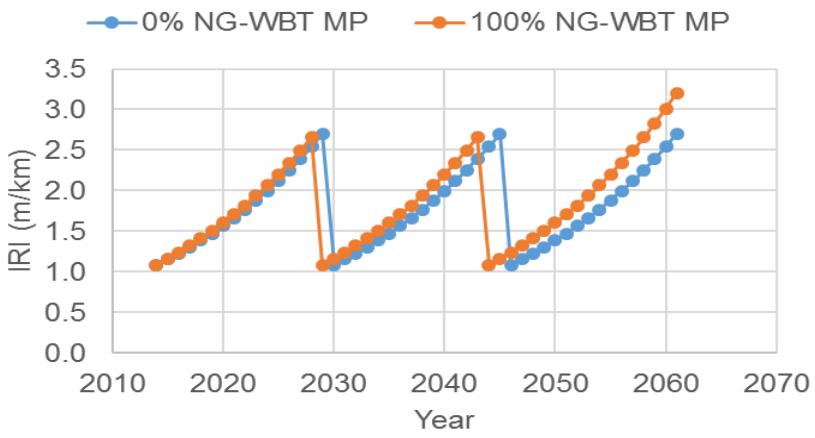

Figure F- 3. Comparison of IRI progression for 0% and 100% NGWBT market penetration based on Scenario 3 SS and the low traffic level (Starting Year = 2014).

APPENDIX G:

LCA RESULTS FOR DIFFERENT BASE/SUBBASE STRENGTHS

ENERGY CONSUMPTION AND GWP FOR THE LOW TRAFFIC LEVEL

From Figure G- 1 to Figure G- 4, the impact of material, construction, maintenance, and rolling resistance is constant regardless of the strength of base and subbase; however, the fuel savings from NGWBT are changing with respect to market penetration. From Figure G- 5 to Figure G- 8, the impact of each life-cycle stage and rolling resistance changes with the IRI progression, which triggers pavement rehabilitation at slightly different time; therefore, the result of LCA analysis varies slightly with different base and subbase strengths ("WW", "MM", "MW", and "MS" refer to "weak base & weak subbase", "medium base & medium subbase", "medium base & weak subbase", and "medium base & strong subbase", respectively in the following figures).

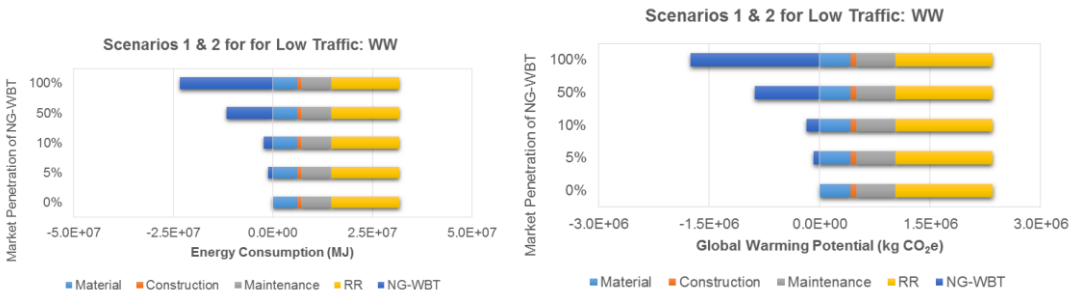

Figure G- 1. Energy consumption and GWP for Scenarios 1 & 2 WW based on the low traffic level.

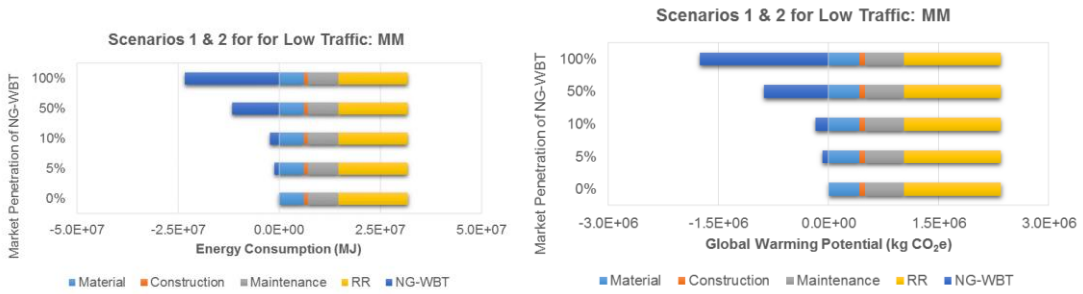

Figure G- 2. Energy consumption and GWP for Scenarios 1 & 2 MM based on the low traffic level.

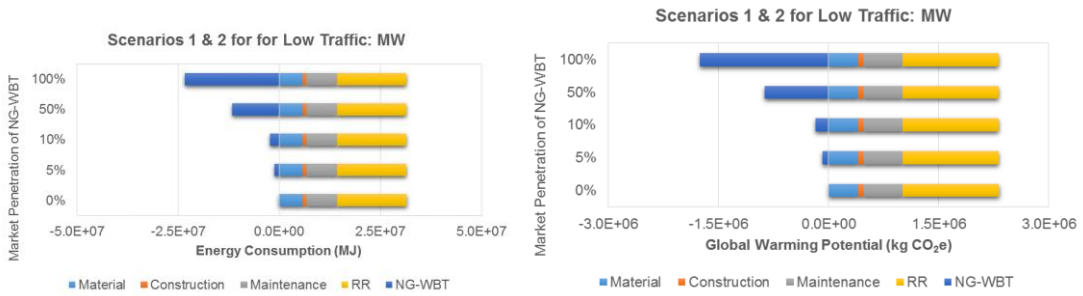

Figure G- 3. Energy consumption and GWP for Scenarios 1 & 2 MW based on the low traffic level.

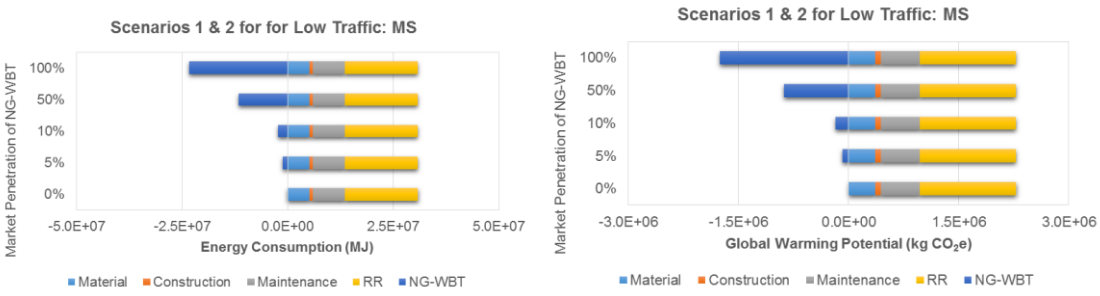

Figure G- 4. Energy consumption and GWP for Scenarios 1 & 2 MS based on the low traffic level.

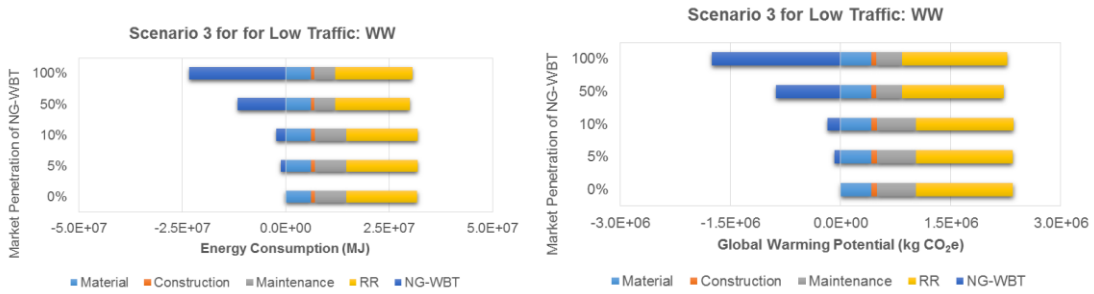

Figure G- 5. Energy consumption and GWP for Scenario 3 WW based on the low traffic level.

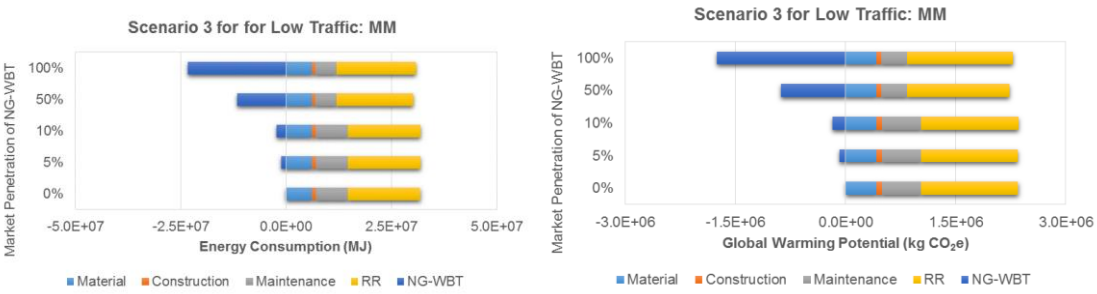

Figure G- 6. Energy consumption and GWP for Scenario 3 MM based on the low traffic level.

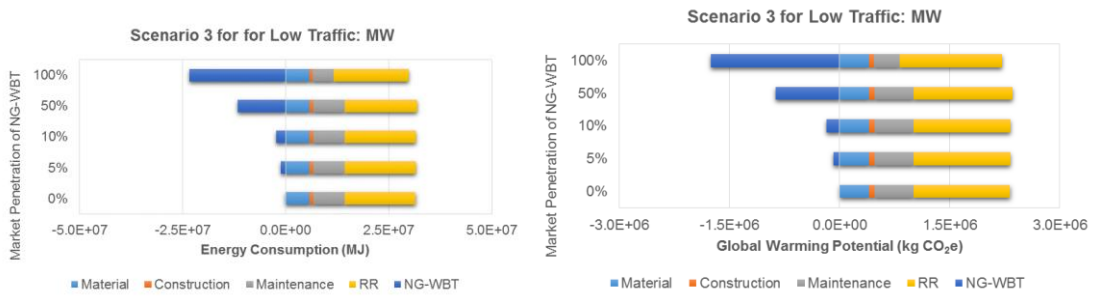

Figure G- 7. Energy consumption and GWP for Scenario 3 MW based on the low traffic level.

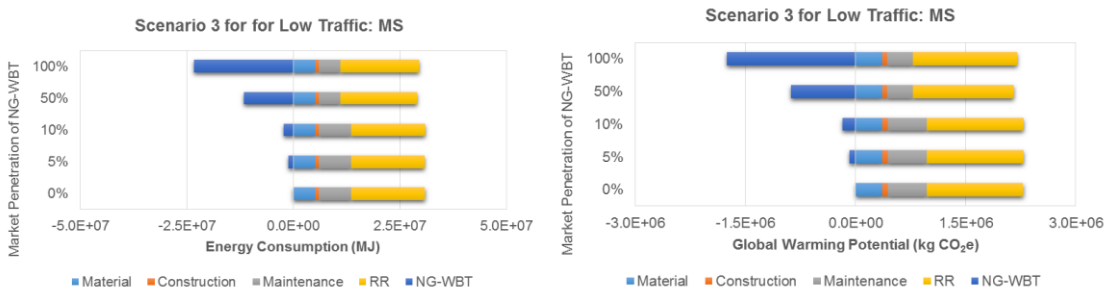

Figure G- 8. Energy consumption and GWP for Scenario 3 MS based on the low traffic level.

ENERGY CONSUMPTION AND GWP FOR THE HIGH TRAFFIC LEVEL

From Figure G- 9 to Figure G- 12, similar to the low traffic level, the impact of material, construction, maintenance, and rolling resistance remains the same but the fuel saving from NGWBT changes with NGWBT market penetration. Figure G- 13 through Figure G- 16 indicates that pavement rehabilitation is triggered primarily by the bottom-up fatigue cracking. At higher market penetration of NGWBT, the pavement life significantly decreases so more frequent rehabilitations are applied during the analysis period; this increases the burden from material production and equipment operation but significantly reduces the impact of rolling resistance because the roughness level is kept lower from frequent rehabilitations. In Figure G- 17 through Figure G- 20, pavement rehabilitation is triggered by IRI. Since rutting potential influences IRI progression, at higher market penetration, rehabilitation is triggered slightly earlier, resulting in the reduction of the overall pavement roughness during the analysis period. This causes a reduction in the impact of rolling resistance at higher market penetration. For all cases, the fuel savings from using NGWBT are considered (“WW”, “MM”, “MW”, and “MS” refer to “weak base & weak subbase”, “medium base & medium subbase”, “medium base & weak subbase”, and “medium base & strong subbase”, respectively in the following figures).

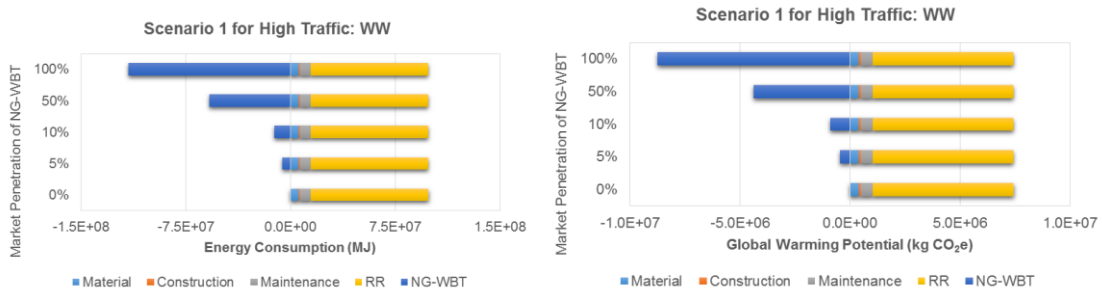

Figure G- 9. Energy consumption and GWP for Scenario 1 WW based on the high traffic level.

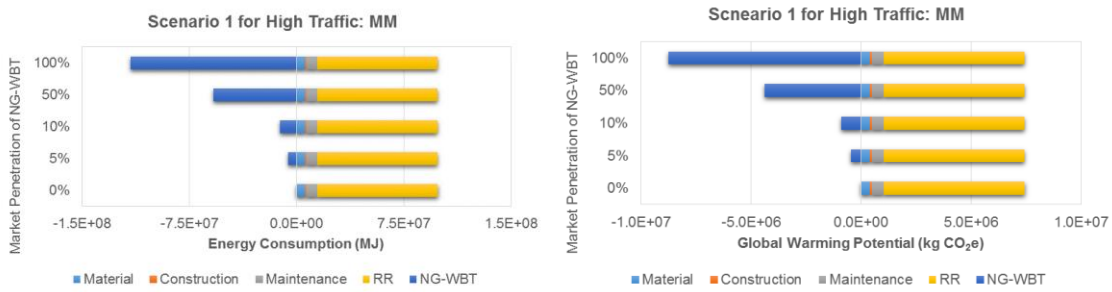

Figure G- 10. Energy consumption and GWP for Scenario 1 MM based on the high traffic level.

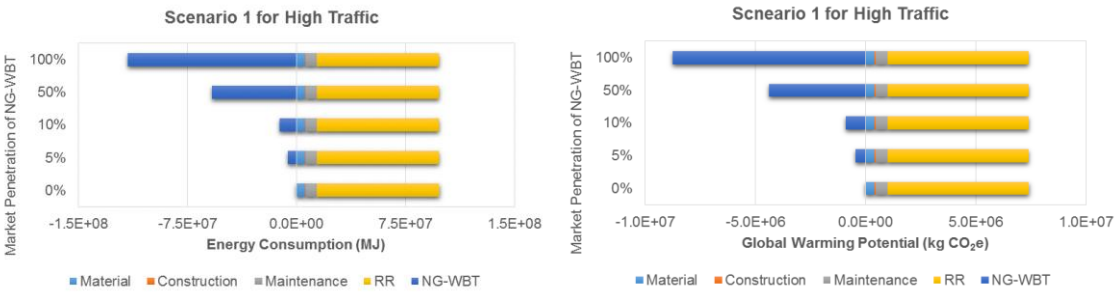

Figure G- 11. Energy consumption and GWP for Scenario 1 MW based on the high traffic level.

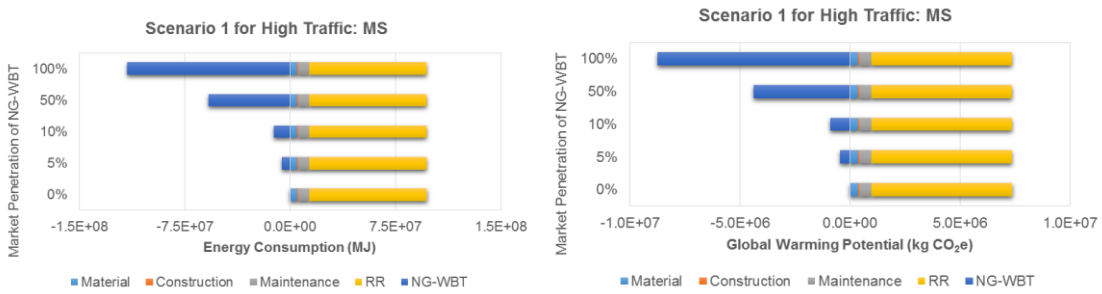

Figure G- 12. Energy consumption and GWP for Scenario 1 MS based on the high traffic level.

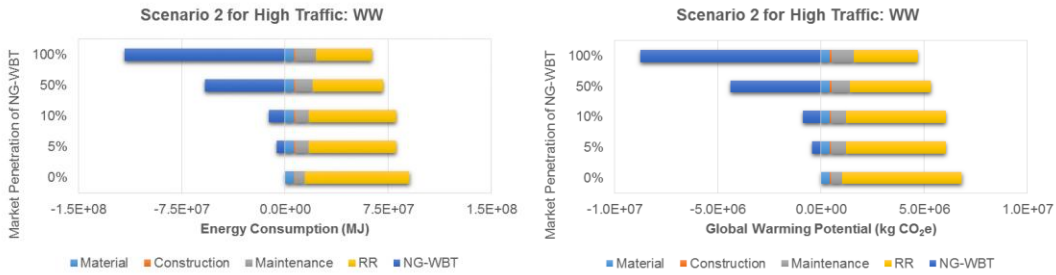

Figure G- 13. Energy consumption and GWP for Scenario 2 WW based on the high traffic level.

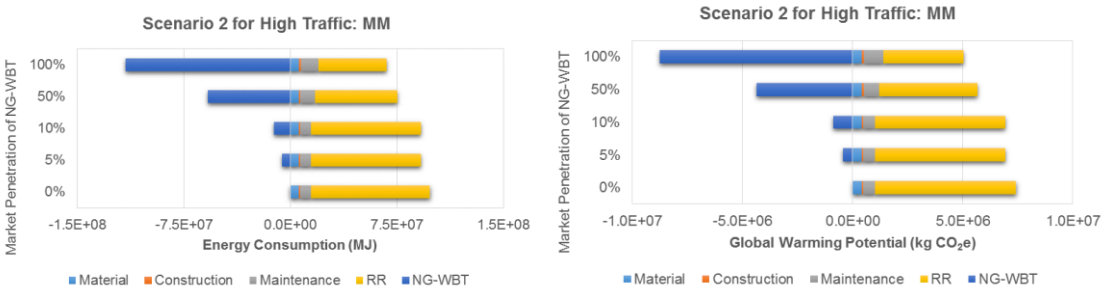

Figure G- 14. Energy consumption and GWP for Scenario 2 MM based on the high traffic level.

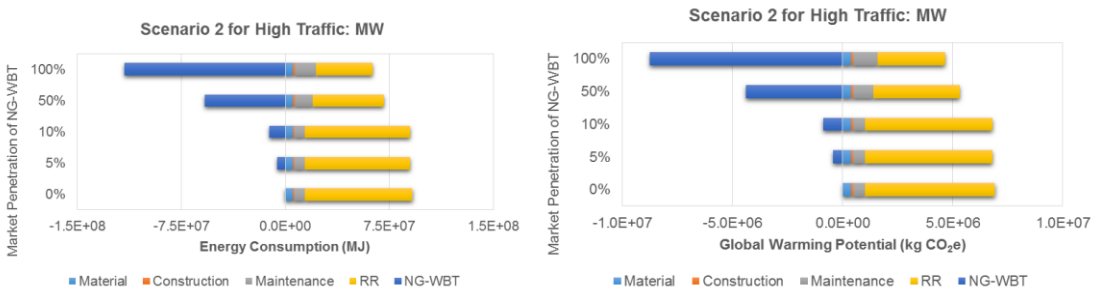

Figure G- 15. Energy Consumption and GWP for Scenario 2 MW based on the high traffic level.

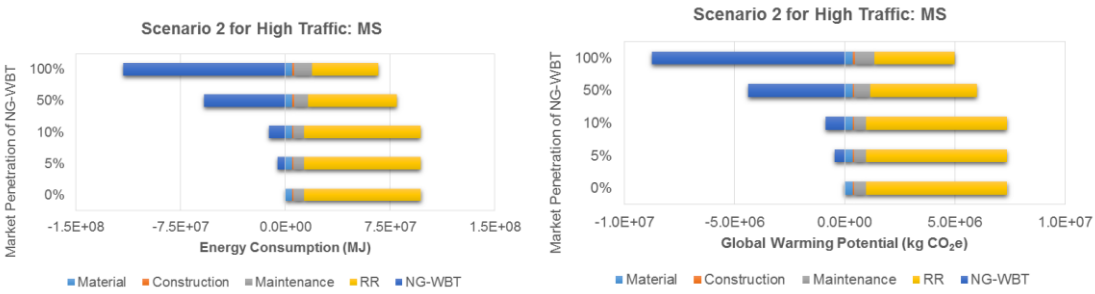

Figure G- 16. Energy consumption and GWP for Scenario 2 MS based on the high traffic level.

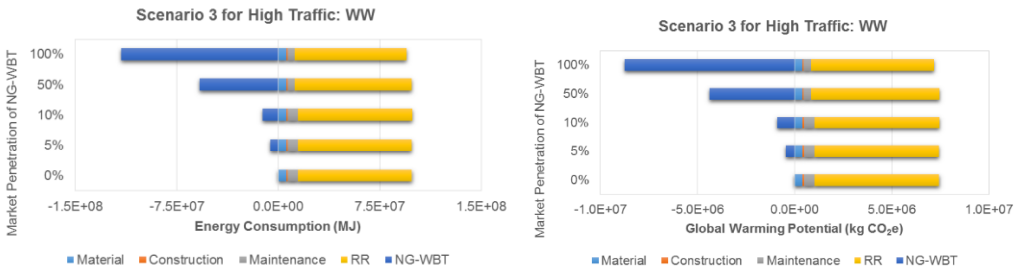

Figure G- 17. Energy consumption and GWP for Scenario 3 WW based on the high traffic level.

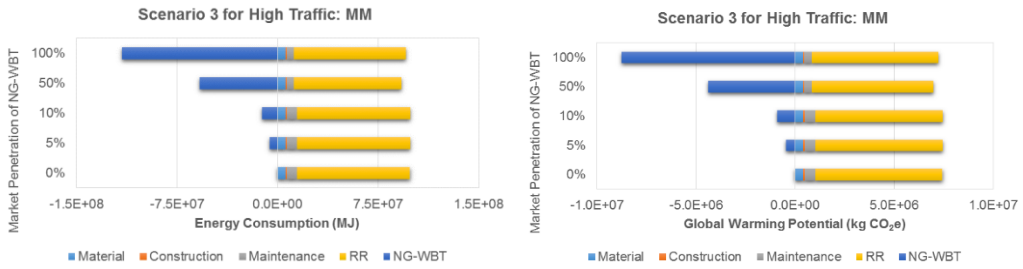

Figure G- 18. Energy consumption and GWP for Scenario 3 MM based on the high traffic level.

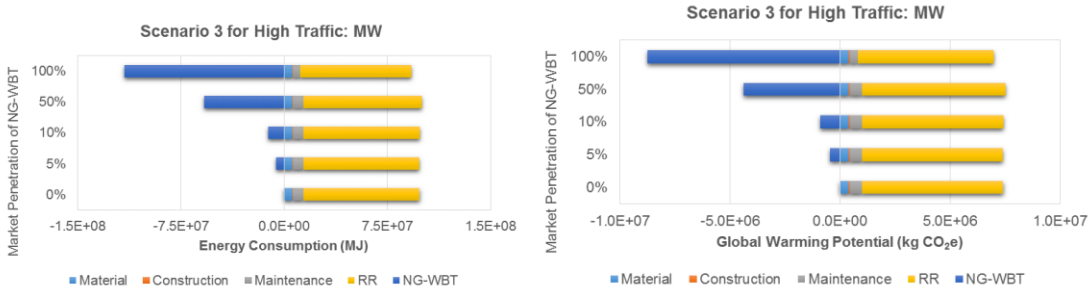

Figure G- 19. Energy consumption and GWP for Scenario 3 MW based on the high traffic level.

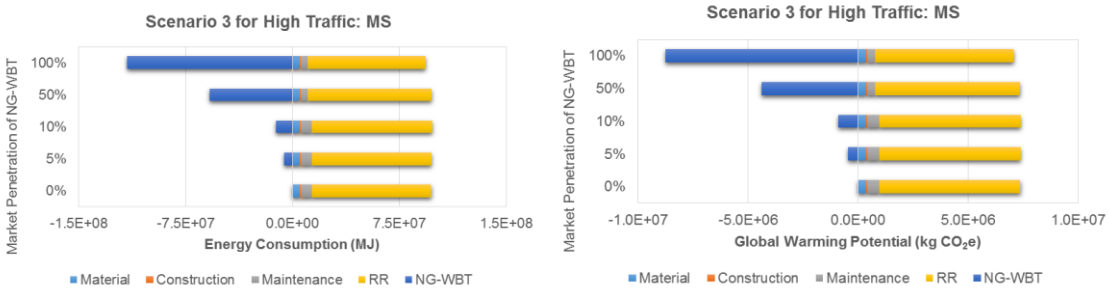

Figure G- 20. Energy consumption and GWP for Scenario 3 MS based on the high traffic level.

APPENDIX H:

SENSITIVITY ANALYSIS BASED ON PERCENTAGE AXLES EQUIPPED WITH NGWBT

For 50% axle with NGWBT, as small trucks have only one axle to be equipped with NGWBT, 0% axle with NGWBT is assumed. For medium and high trucks, 50% axle with NGWBT is assumed; one axle in medium trucks and two axles in heavy trucks are equipped with NGWBT. For 100% axle with NGWBT, all axles except for driving axle are equipped with NGWBT. “SS” refers to “strong base and strong subbase” in the following figures.

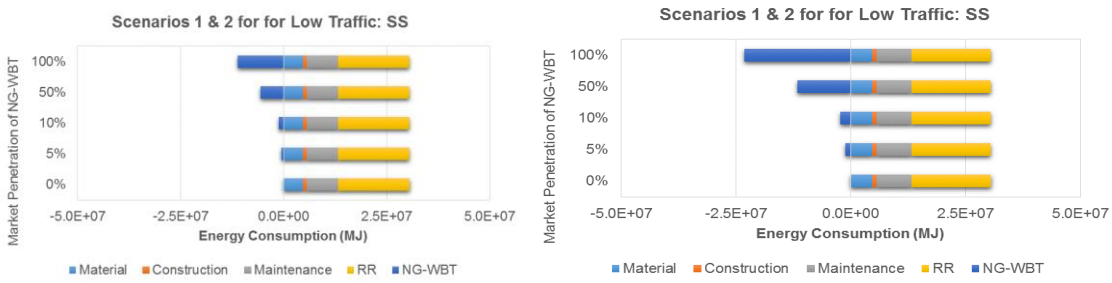

Figure H- 1. Comparison of energy consumption for: 50% (left) and 100% (right) axle with NGWBT based on Scenarios 1 & 2 SS and the low traffic level.

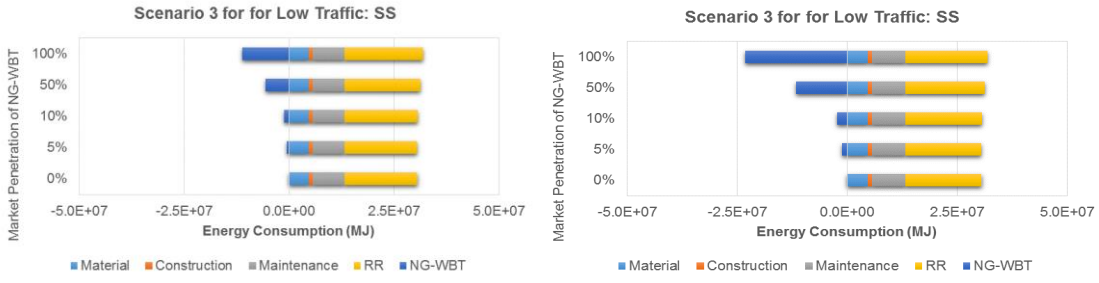

Figure H- 2. Comparison of energy consumption for: 50% (left) and 100% (right) axle with NGWBT based on Scenario 3 SS and the low traffic level.

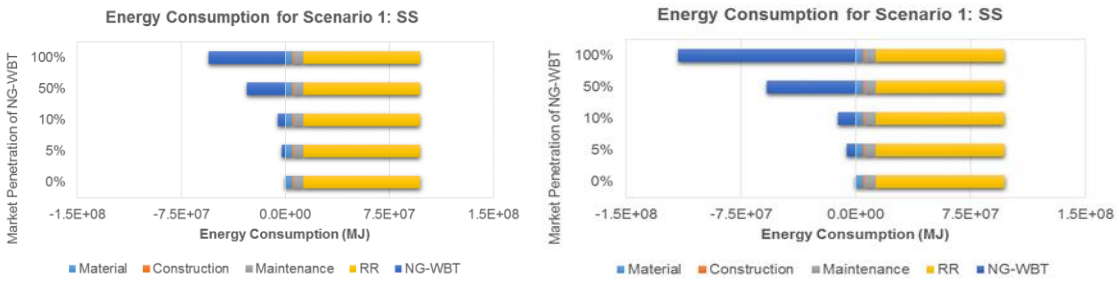

Figure H- 3. Comparison of energy consumption for (a) 50% and (b) 100% axle with NGWBT based on Scenario 1 SS and the high traffic level.

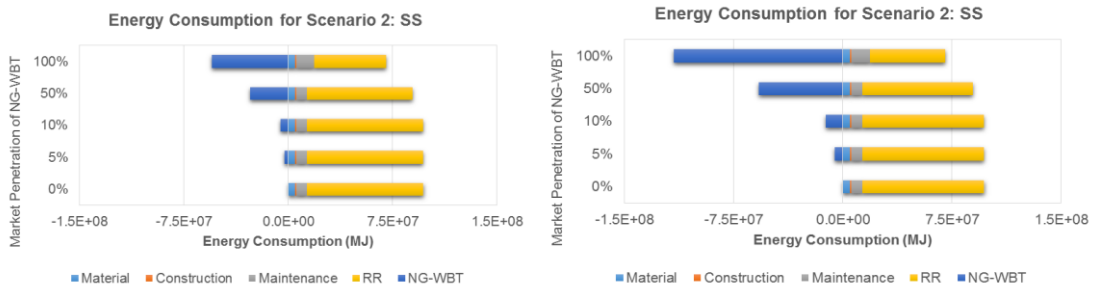

Figure H- 4. Comparison of energy consumption for 50% (left) and 100% (right) axle with NGWBT based on Scenario 2 SS and the high traffic level.

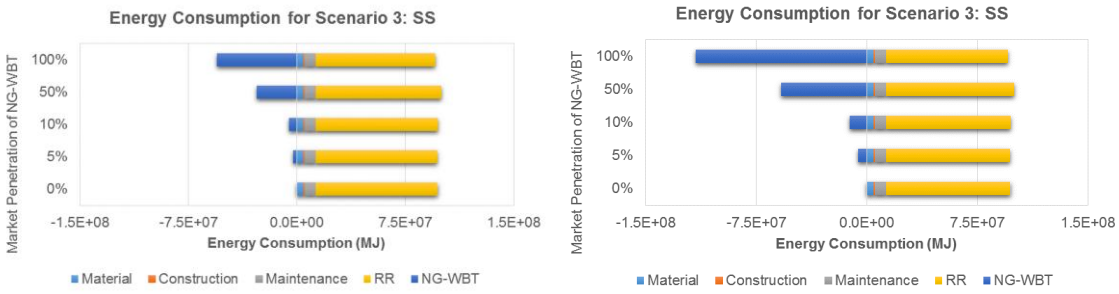

Figure H- 5. Comparison of energy consumption for 50% (left) and 100% (right) axle with NGWBT based on Scenario 3 SS and the high traffic level.